Title
The metabolite α-ketoglutarate extends lifespan by inhibiting ATP synthase and TOR

Journal
Nature, 510(7505)

ISSN
0028-0836

Authors
Chin, Randall M
Fu, Xudong
Pai, Melody Y
et al.

Publication Date
2014-06-01

DOI
10.1038/nature13264

Peer reviewed

Published in final edited form as:
Nature. 2014 June 19; 510(7505): 397–401. doi:10.1038/nature13264.

The metabolite alpha-ketoglutarate extends lifespan by inhibiting the ATP synthase and TOR

Randall M. Chin[1], **Xudong Fu**[2], **Melody Y. Pai**[1,*], **Laurent Vergnes**[3,*], **Heejun Hwang**[2,*], **Gang Deng**[4], **Simon Diep**[2], **Brett Lomenick**[2], **Vijaykumar S. Meli**[5], **Gabriela C. Monsalve**[5], **Eileen Hu**[2], **Stephen A. Whelan**[6], **Jennifer X. Wang**[7], **Gwanghyun Jung**[2], **Gregory M. Solis**[8], **Farbod Fazlollahi**[9], **Chitrada Kaweeteerawat**[10], **Austin Quach**[2], **Mahta Nili**[11], **Abby S. Krall**[2], **Hilary A. Godwin**[10], **Helena R. Chang**[6], **Kym F. Faull**[9], **Feng Guo**[5], **Meisheng Jiang**[2], **Sunia A. Trauger**[7], **Alan Saghatelian**[12], **Daniel Braas**[2,13], **Heather R. Christofk**[2,13], **Catherine F. Clarke**[1,4], **Michael A. Teitell**[1,11], **Michael Petrascheck**[8], **Karen Reue**[1,3], **Michael E. Jung**[1,4], **Alison R. Frand**[5], and **Jing Huang**[1,2]

[1]Molecular Biology Institute, University of California Los Angeles, Los Angeles, CA

[2]Department of Molecular and Medical Pharmacology, University of California Los Angeles, Los Angeles, CA

[3]Department of Human Genetics, University of California Los Angeles, Los Angeles, CA

[4]Department of Chemistry and Biochemistry, University of California Los Angeles, Los Angeles, CA

[5]Department of Biological Chemistry, University of California Los Angeles, Los Angeles, CA

[6]Department of Surgery, University of California Los Angeles, Los Angeles, CA

[7]Small Molecule Mass Spectrometry Facility, FAS Division of Science, Harvard University, Cambridge, MA

[8]Department of Chemical Physiology, The Scripps Research Institute, La Jolla, CA

[9]Pasarow Mass Spectrometry Laboratory, Department of Psychiatry and Biobehavioral Sciences and Semel Institute for Neuroscience and Human Behavior, University of California Los Angeles, Los Angeles, CA

[10]Department of Environmental Health Sciences, University of California Los Angeles, Los Angeles, CA

Correspondence to J.H. (jinghuang@mednet.ucla.edu).
*These authors contributed equally to this work

Supplementary Information is linked to the online version of the paper at www.nature.com/nature.

Author Contributions Lifespan assays were performed by R.M.C., M.P., and E.H.; DARTS-MS by S.D. and B.L.; DARTS-Western by M.Y.P., H.H., and R.M.C.; mammalian cell experiments by X.F. and H.H.; mitochondrial respiration study design and analyses by L.V. and K.R.; enzyme kinetics and analyses by R.M.C. and J.H.; confocal microscopy by V.S.M., G.C.M., and A.R.F.; UHPLC-ESI/MS/MS by J.X.W. and S.A.T.; compound syntheses by G.D. and M.E.J.; other analyses by H.H., X.F., M.Y.P., D.B., R.M.C., E.H., G.J., G.M.S., C.K., and A.Q. S.A.W., F.F., M.N., A.S.K., H.A.G., H.R.C., K.F.F., F.G., M.J., S.A.T., A.S., D.B., H.R.C., C.F.C., M.A.T., M.E.J., L.V., K.R., A.R.F., and M.P. provided guidance, specialized reagents, and expertise. J.H. conceived the study. R.M.C. and J.H. wrote the paper. R.M.C., X.F., and J.H. analysed data. All authors discussed the results, commented on the studies, and contributed to aspects of preparing the manuscript.

The authors declare no competing financial interests.

[11]Department of Pathology and Laboratory Medicine, University of California Los Angeles, Los Angeles, CA

[12]Department of Chemistry and Chemical Biology, Harvard University, Cambridge, MA

[13]UCLA Metabolomics Center, University of California Los Angeles, Los Angeles, CA

Abstract

Metabolism and ageing are intimately linked. Compared to ad libitum feeding, dietary restriction (DR) or calorie restriction (CR) consistently extends lifespan and delays age-related diseases in evolutionarily diverse organisms[1,2]. Similar conditions of nutrient limitation and genetic or pharmacological perturbations of nutrient or energy metabolism also have longevity benefits[3,4]. Recently, several metabolites have been identified that modulate ageing[5,6] with largely undefined molecular mechanisms. Here we show that the tricarboxylic acid (TCA) cycle intermediate α-ketoglutarate (α-KG) extends the lifespan of adult *C. elegans*. ATP synthase subunit beta is identified as a novel binding protein of α-KG using a small-molecule target identification strategy called DARTS (drug affinity responsive target stability)[7]. The ATP synthase, also known as Complex V of the mitochondrial electron transport chain (ETC), is the main cellular energy-generating machinery and is highly conserved throughout evolution[8,9]. Although complete loss of mitochondrial function is detrimental, partial suppression of the ETC has been shown to extend *C. elegans* lifespan[10–13]. We show that α-KG inhibits ATP synthase and, similar to ATP synthase knockdown, inhibition by α-KG leads to reduced ATP content, decreased oxygen consumption, and increased autophagy in both *C. elegans* and mammalian cells. We provide evidence that the lifespan increase by α-KG requires ATP synthase subunit beta and is dependent on the target of rapamycin (TOR) downstream. Endogenous α-KG levels are increased upon starvation and α-KG does not extend the lifespan of DR animals, indicating that α-KG is a key metabolite that mediates longevity by DR. Our analyses uncover new molecular links between a common metabolite, a universal cellular energy generator, and DR in the regulation of organismal lifespan, thus suggesting new strategies for the prevention and treatment of ageing and age-related diseases.

To gain insight into the regulation of ageing by endogenous small molecules, we screened normal metabolites and aberrant disease-associated metabolites for their effects on the adult lifespan using the *C. elegans* model. We discovered that the TCA cycle intermediate α-KG (but not isocitrate or citrate) delays ageing and extends the lifespan of *C. elegans* by ~50% (Fig. 1a, Extended Data Fig. 1a). In the cell, α-KG (or 2-oxoglutarate, Fig. 1b) is produced from isocitrate by oxidative decarboxylation catalyzed by isocitrate dehydrogenase (IDH). α-KG can also be produced anaplerotically from glutamate by oxidative deamination using glutamate dehydrogenase, and as a product of pyridoxal phosphate-dependent transamination reactions where glutamate is a common amino donor. α-KG extended wildtype N2 lifespan in a concentration-dependent manner, with 8 mM α-KG producing the maximal lifespan extension (Fig. 1c); 8 mM was the concentration used in all subsequent *C. elegans* experiments. There is a ~50% increase in α-KG concentration in worms on 8 mM α-KG plates compared to those on vehicle plates (Extended Data Fig. 1b), or ~160 μM vs. ~110 μM assuming homogenous distribution (Methods). α-KG not only extends lifespan, but also delays age-related phenotypes, such as the decline in rapid, coordinated body

movement (Supplementary Videos 1–2). α-KG supplementation in the adult stage is sufficient for longevity (Extended Data Fig. 1c).

The dilution or killing of the bacterial food has been shown to extend worm lifespan[14], but the lifespan increase by α-KG is not due to altered bacterial proliferation or metabolism (Fig. 1d–e, Extended Data Fig. 1d). Animals also did not view α-KGtreated food as less favorable (Extended Data Fig. 1e–f), and there was no significant change in food intake, pharyngeal pumping, foraging behavior, body size, or brood size in the presence of α-KG (Extended Data Fig. 1e–h, data not shown).

In the cell, α-KG is decarboxylated to succinyl-CoA and CO_2 by α-KG dehydrogenase (encoded by *ogdh-1*), a key control point in the TCA cycle. Increasing α-KG levels by *ogdh-1* RNAi (Extended Data Fig. 1b) also extends worm lifespan (Fig. 1f; Supplementary Notes), consistent with a direct effect of α-KG on longevity independent of the bacterial food.

To investigate the molecular mechanism(s) of longevity by α-KG, we took advantage of an unbiased biochemical approach, DARTS[7]. Since we hypothesized that key target(s) of α-KG are likely to be conserved and ubiquitously expressed, we used a human cell line (Jurkat) that is easy to culture as the protein source for DARTS (Fig. 2a). Mass spectrometry identified ATP5B, the beta subunit of the catalytic core of the ATP synthase, among the most abundant and enriched proteins present in the α-KG treated sample (Extended Data Table 1); the homologous alpha subunit ATP5A was also enriched albeit to a lesser extent. The interaction between α-KG and ATP5B was verified using additional cell lines (Fig. 2b, data not shown), and corroborated for the *C. elegans* ortholog ATP-2 (Extended Data Fig. 2a).

α-KG inhibits the activity of Complex V, but not Complex IV, from bovine heart mitochondria (Fig. 2c, Extended Data Fig. 2b, data not shown). This inhibition is also readily detected in live mammalian cells (Fig. 2d, data not shown) and in live nematodes (Fig. 2e), as evidenced by the reduced ATP levels. Concomitantly, oxygen consumption rates are lowered (Fig. 2f–g), similar to the scenario with *atp-2* knockdown (Extended Data Fig. 2c). Specific inhibition of Complex V, but not the other ETC complexes, by α-KG is further confirmed by respiratory control analysis[15] (Fig. 2h, Extended Data Fig. 2d–h). To understand the mechanism of inhibition by α-KG, we studied the enzyme inhibition kinetics of ATP synthase. α-KG (released from octyl α-KG) decreases both the effective V_{max} and K_m of ATP synthase, indicative of uncompetitive inhibition (Fig. 2i, Supplementary Notes).

To determine the significance of ATP-2 to the longevity by α-KG, we measured the lifespan of *atp-2(RNAi)* adults given α-KG. As reported[13], *atp-2(RNAi)* animals live longer (Fig. 3a). However, their lifespan is not further extended by α-KG (Fig. 3a), indicating that ATP-2 is required for the longevity benefit of α-KG. This requirement is specific because, in contrast, the lifespan of the even longer-lived insulin/IGF-1 receptor *daf-2(e1370)* mutant worms[3] is further increased by α-KG (Fig. 3b). Remarkably, oligomycin, an inhibitor of ATP synthase, also extends the lifespan of adult worms (Extended Data Fig. 3a). Together, the direct binding of ATP-2 by α-KG, the related enzymatic inhibition, reduction in ATP levels and

oxygen consumption, lifespan analysis, and other similarities (see also Supplementary Notes, Extended Data Fig. 4) to *atp-2* knockdown or oligomycin treatment demonstrate that α-KG likely extends lifespan primarily by targeting ATP-2.

The lower ATP content in α-KG treated animals suggests that longevity by α-KG may involve a DR-like state. Consistent with this idea, we found that α-KG does not extend the lifespan of *eat-2(ad1116)* animals (Fig. 3c), which is a model of DR with impaired pharyngeal pumping and therefore reduced food intake[16]. The longevity of *eat-2* mutants requires TOR/*let-363*[17], an important mediator of the effects of DR on longevity[18]. Likewise, α-KG fails to increase the lifespan of *CeTOR(RNAi)* animals (Fig. 3d). The AMP-activated protein kinase (AMPK) is another conserved major sensor of cellular energy status[19]. Both AMPK/*aak-2* and the FoxO transcription factor DAF-16 mediate DR-induced longevity in *C. elegans* fed diluted bacteria[20], but neither is required for lifespan extension in the *eat-2* model[16,20]. We found that in *aak-2* (Extended Data Fig. 5a) and *daf-16* (Fig. 3e) mutants the longevity effect of α-KG is smaller than in N2 ($P < 0.0001$), suggesting that α-KG longevity partially depends on AMPK and FoxO; nonetheless, lifespan is significantly increased by α-KG in *aak-2* (24.3%, $P < 0.0001$) and *daf-16* (29.5%, $P < 0.0001$) mutant or RNAi animals (Fig. 3e, Extended Data Fig. 5a–b, data not shown), indicating an AMPK-FoxO independent effect by α-KG in longevity.

The inability of α-KG to further extend the lifespan of *CeTOR(RNAi)* animals suggests that α-KG treatment and TOR inactivation extend lifespan either through the same pathway (with α-KG acting on or upstream of TOR), or through independent mechanisms or parallel pathways that converge on a downstream effector. The first model predicts that the TOR pathway will be less active upon α-KG treatment, whereas if the latter model were true then TOR would be unaffected by α-KG treatment. In support of the first model, we found that TOR pathway activity is decreased in human cells treated with octyl α-KG (Fig. 4a, Extended Data Fig. 6a–b). However, α-KG does not interact with TOR directly (Extended Data Fig. 6d–e). Consistent with the involvement of TOR in α-KG longevity, the FoxA transcription factor PHA-4, which is required to extend adult lifespan in response to reduced CeTOR signaling[21] and for DR-induced longevity in *C. elegans*[22], is likewise required for α-KG-induced longevity (Fig. 3f). Moreover, autophagy, which is activated both by TOR inhibition[18,23] and by DR[24], is markedly increased in worms treated with α-KG (or *ogdh-1* RNAi) and in *atp-2(RNAi)* animals (Fig. 4b–c, Extended Data Fig. 6c, Extended Data Fig. 7, Supplementary Notes), as indicated by the prevalence of GFP::LGG-1 puncta (Methods). Autophagy was also induced in mammalian cells treated with octyl α-KG (Extended Data Fig. 6f). Furthermore, α-KG does not result in significantly more autophagy in either *atp-2(RNAi)* or *CeTOR(RNAi)* worms (Fig. 4b–c). The data provide further evidence that α-KG decreases TOR pathway activity through the inhibition of ATP synthase. Similarly, autophagy is induced by oligomycin, and oligomycin does not augment autophagy in *CeTOR(RNAi)* worms (Extended Data Fig. 3b–c).

α-KG is not only a metabolite, but also a co-substrate for a large family of dioxygenases[25]. The hypoxia inducible factor (HIF-1) is modified by one of these enzymes, the prolyl 4-hydroxylase (PHD) EGL-9, and thereafter degraded by the von Hippel-Lindau (VHL) protein[26,27]. α-KG extends the lifespan of animals with loss-offunction mutations in *hif-1*,

egl-9, and *vhl-1* (Fig. 3g, Extended Data Fig. 5c), suggesting that this pathway does not play a major role in lifespan extension by α-KG. However, it is prudent to acknowledge that the formal possibility of other α-KG binding targets playing an additional role in the extension of lifespan by α-KG cannot be eliminated at this time.

In summary, we show that ageing in *C. elegans* is delayed by α-KG supplementation to adult animals. This longevity effect is likely mediated by the ATP synthase, which we identified as a direct target of α-KG, and TOR, a major effector of DR. Identification of new protein targets of α-KG illustrates that regulatory networks acted upon by the metabolites are likely more complex than currently appreciated, and that DARTS is a useful method for discovering new protein targets and regulatory functions of metabolites. Our findings demonstrate a novel mechanism for extending lifespan that is mediated by the regulation of cellular energy metabolism by a key metabolite. Such moderation of ATP synthesis by metabolite(s) has likely evolved to ensure energy efficiency by the organism in response to nutrient availability. We suggest that this system may be exploited to confer a DR-like state that favors maintenance over growth, and thereby delay ageing and prevent age-related diseases. In fact, the TOR pathway is often hyperactivated in human cancer; inhibition of TOR function by α-KG in normal human cells suggests an exciting role for α-KG as an endogenous tumor suppressor metabolite. Interestingly, physiological increases in α-KG levels have been reported in starved yeast and bacteria[28], in the liver of starved pigeons[29], and in humans after physical exercise[30]. The biochemical basis for this increase of α-KG is explained by starvation-based anaplerotic gluconeogenesis, which activates glutamate-linked transaminases in the liver to provide carbon derived from amino acid catabolism. Consistent with this idea, α-KG levels are elevated in starved *C. elegans* (Fig. 4d). These findings suggest a model in which α-KG is a key metabolite mediating lifespan extension by starvation/DR (Fig. 4e).

Longevity molecules that delay ageing and extend lifespan have profound implications and have long been a dream of humanity. Endogenous metabolites such as α-KG that can alter *C. elegans* lifespan suggest that an internal mechanism may exist that is accessible to a myriad of regulations and interventions.

METHODS

Nematode strains and maintenance

Caenorhabditis elegans strains were maintained using standard methods[31]. The following strains were used.

Strain	Genotype	Source
Bristol N2	wildtype	*Caenorhabditis* Genetics Center (CGC), University of Minnesota
DA1116	*eat-2(ad1116)*II	CGC
CB1370	*daf-2(e1370)*III	CGC
CF1038	*daf-16(mu86)*I	CGC

Strain	Genotype	Source
PD8120	*smg-1(cc546ts)*I	CGC
SM190	*smg-1(cc546ts)*I;*pha-4(zu225)*V	CGC
RB754	*aak-2(ok524)*X	CGC
ZG31	*hif-1(ia4)*V	CGC
ZG596	*hif-1(ia7)*V	CGC
JT307	*egl-9(sa307)*V	CGC
CB5602	*vhl-1(ok161)*X	CGC
DA2123	*adIs2122[lgg-1*::*GFP + rol-6(su1006)]*	CGC

RNAi in *C. elegans*

RNAi in *C. elegans* was accomplished by feeding worms HT115(DE3) bacteria expressing target-gene double-stranded RNA (dsRNA) from the pL4440 vector[32]. dsRNA production was induced overnight on plates containing 1 mM IPTG. All RNAi feeding clones were obtained from the *C. elegans* ORF-RNAi Library (Thermo Scientific/Open Biosystems) unless otherwise stated. The *C. elegans* TOR (CeTOR) RNAi clone[33] was obtained from Joseph Avruch (MGH/Harvard). Efficient knockdown was confirmed by Western blotting of the corresponding protein or by qRT-PCR of the mRNA. The primer sequences used for qRT-PCR are as follows.

atp-2 forward: TGACAACATTTTCCGTTTCACC

atp-2 reverse: AAATAGCCTGGACGGATGTGAT

let-363/CeTOR forward: GATCCGAGACAAGATGAACGTG

let-363/CeTOR reverse: ACAATTTGGAACCCAACCAATC

ogdh-1 forward: TGATTTGGACCGAGAATTCCTT

ogdh-1 reverse: GGATCAGACGTTTGAACAGCAC

We validated the RNAi knockdown of both *ogdh-1* and *atp-2* by quantitative RT-PCR and also of *atp-2* by Western blotting. Transcripts of *ogdh-1* were reduced by 85%, and transcripts and protein levels of *atp*-2 were reduced by 52% and 83%, respectively, in larvae that were cultivated on bacteria that expressed the corresponding dsRNAs. In addition, RNAi of *atp-2* in our hands was associated with delayed post-embryonic development and larval arrest, consistent with the phenotypes of *atp-2(ua2)* animals. Analysis by qRT-PCR indicated a modest but significant decrease by 26% in transcripts of *CeTOR* in larvae undergoing RNAi; moreover, molecular markers for autophagy were induced in these animals, and the lifespan of adults was extended, consistent with partial inactivation of the kinase.

In lifespan experiments, we used RNAi to inactivate *atp-2*, *ogdh-1*, and *CeTOR* in mature animals in the presence or absence of exogenous α-KG. The concentration of α-KG used in these experiments (8 mM) was empirically determined to be most beneficial for wild-type animals (Fig. 1c). This approach enabled us to evaluate the contribution of essential proteins

and pathways to the longevity conferred by supplemental α-KG. Specifically, we were able to substantially but not fully inactivate *atp-2* in adult animals that had completed embryonic and larval development. As described in our manuscript, supplementation with 8 mM α-KG did not further extend (and in fact, in one occasion, even decreased) the lifespan of *atp-2(RNAi)* animals (Extended Data Table 2), indicating that *atp-2* is required for α-KG to promote longevity. On the other hand, a complete inactivation of *atp-2* would be lethal, and thereby mask the benefit of ATP synthase inhibition by α-KG.

Lifespan analysis

Lifespan assays were conducted at 20 °C on solid nematode growth media (NGM) using standard protocols and were replicated in at least two independent experiments. *C. elegans* were synchronized by performing either a timed egg lay[34] or an egg preparation (lysing ~100 gravid worms in 70 μl M9 buffer[31], 25 μl bleach (10% sodium hypochlorite solution), and 5 μl 10 N NaOH). Young adult animals were picked onto NGM assay plates containing 1.5% dimethyl sulfoxide (DMSO; Sigma, D8418), 49.5 μM 5-fluoro-2'-deoxyuridine[34] (FUDR; Sigma, F0503), and α-KG (Sigma, K1128) or vehicle control (H_2O). FUDR was included to prevent progeny production. Media containing α-KG were adjusted to pH 6.0 (i.e., the same pH as the control plates) by the addition of NaOH. All compounds were mixed into the NGM media after autoclaving and before solidification of the media. Assay plates were seeded with OP50 (or a designated RNAi feeding clone, see below). Worms were moved to new assay plates every 4 days (to ensure sufficient food was present at all times and to reduce the risk of mold contamination). To assess the survival of the worms, the animals were prodded with a platinum wire every 2–3 days, and those that failed to respond were scored as dead. For analysis concerning mutant strains, the corresponding parent strain was used as a control in the same experiment.

For lifespan experiments involving RNAi, the plates also contained 1 mM isopropyl β-D-1-thiogalactopyranoside (IPTG; Acros, CAS 367-93-1) and 50 μg/mL ampicillin (Fisher, BP1760-25). RNAi was accomplished by feeding N2 worms HT115(DE3) bacteria expressing target-gene dsRNA from pL4440[32]; control RNAi was done in parallel for every experiment by feeding N2 worms HT115(DE3) bacteria expressing either GFP dsRNA or empty vector (which gave identical lifespan results).

Lifespan experiments with oligomycin (Cell signaling, 9996) were performed as described for α-KG (i.e., NGM plates with 1.5% DMSO and 49.5 μM FUDR; N2 worms; OP50 bacteria).

For lifespan experiments concerning *smg-1(cc546ts);pha-4(zu225) and smg-1(cc546ts)*[22,35], from egg to L4 stage the strains were grown from egg to L4 stage at 24°C, which inactivates the *smg-1* temperature-sensitive allele, preventing mRNA surveillance-mediated degradation of the *pha-4(zu225)* mRNA which contains a premature stop codon, and thus produces a truncated but fully functional PHA-4 transcription factor[35]). Then at the L4 stage the temperature was shifted to 20°C, which restores *smg-1* function and thereby results in the degradation of *pha-4(zu225)* mRNA. Treatment with α-KG began at the L4 stage.

All lifespan data are available in Extended Data Table 2, including sample sizes. The sample size was chosen on the basis of standards done in the field in published manuscripts. No statistical method was used to predetermine the sample size. Animals were assigned randomly to the experimental groups. Worms that ruptured, bagged (i.e., exhibited internal progeny hatching), or crawled off the plates were censored. Lifespan data were analyzed using GraphPad Prism; *P*-values were calculated using the log-rank (Mantel-Cox) test.

Statistical analyses

All experiments have been repeated at least two times with identical or similar results. Data represent biological replicates. Appropriate statistical tests are used for every figure. Data meet the assumptions of the statistical tests described for each figure. Mean ± s.d. is plotted in all figures unless stated otherwise.

Food preference assay

Protocol adapted from Abada *et al.*[36]. A 10 cm NGM plate was seeded with two spots of OP50 as shown in extended data figure 1e. After letting the OP50 lawns to dry over 2 days at room temperature, vehicle (H_2O) or α-KG (8 mM) was added to the top of the lawn and allowed to dry over 2 days at room temperature. ~50–100 synchronized adult day 1 worms were placed onto the center of the plate and their preference for either bacterial lawn was recorded after 3 h at room temperature.

Target identification using drug affinity responsive target stability (DARTS)

For unbiased target ID (Fig. 2a), human Jurkat cells were lysed using M-PER (Thermo Scientific, 78501) with the addition of protease inhibitors (Roche, 11836153001) and phosphatase inhibitors[37]. TNC buffer (50 mM Tris-HCl pH 8.0, 50 mM NaCl, 10 mM $CaCl_2$) was added to the lysate and protein concentration was then determined using the BCA Protein Assay kit (Pierce, 23227). Cell lysates were incubated with either vehicle (H_2O) or α-KG for 1 h on ice followed by an additional 20 min at room temperature. Digestion was performed using Pronase (Roche, 10165921001) at room temperature for 30 min and stopped using excess protease inhibitors with immediate transfer to ice. The resulting digests were separated by SDS-PAGE and visualized using SYPRO Ruby Protein Gel Stain (Invitrogen, S12000). The band with increased staining from the α-KG lane (corresponding to potential protein targets that are protected from proteolysis by the binding of α-KG) and the matching area of the control lane were excised, in-gel trypsin digested, and subjected to LC-MS/MS analysis as described[7,38]. Mass spectrometry results were searched against the human Swissprot database (release 57.15) using Mascot version 2.3.0, with all peptides meeting a significance threshold of 0.05.

For target verification by DARTS-Western blotting (Fig. 2b), HeLa cells were lysed in M-PER buffer (Thermo Scientific, 78501) with the addition of protease inhibitors (Roche, 11836153001) and phosphatase inhibitors (50 mM NaF, 10 mM β-glycerophosphate, 5 mM sodium pyrophosphate, 2 mM Na_3VO_4). Chilled TNC buffer (50 mM Tris-HCl pH 8.0, 50 mM NaCl, 10 mM $CaCl_2$) was added to the protein lysate, and protein concentration of the lysate was measured by the BCA Protein Assay kit (Pierce, 23227). The protein lysate was then incubated with vehicle control (H_2O) or varying concentrations of α-KG for 3 h at

room temperature with shaking at 600 rpm in an Eppendorf Thermomixer. Pronase (Roche, 10165921001) digestions were performed for 20 min at room temperature, and stopped by adding SDS loading buffer and immediately heating at 70 °C for 10 min. Samples were subjected to SDS-PAGE on 4–12% Bis-Tris gradient gel (Invitrogen, NP0322BOX) and Western blotted for ATP synthase subunits ATP5B (Sigma, AV48185), ATP5O (Abcam, ab91400), and ATP5A (Abcam, ab110273). Binding between α-KG and PHD-2/Egln1 (Cell Signaling, 4835), for which α-KG is a co-substrate[39], was confirmed by DARTS. GAPDH (Ambion, AM4300) was used as a negative control.

For DARTS using *C. elegans* (Extended Data Fig. 2a), wildtype animals of various ages were grown on NGM/OP50 plates, washed 4 times with M9 buffer, and immediately placed in the −80 °C freezer. Animals were lysed in HEPES buffer (40 mM HEPES pH 8.0, 120 mM NaCl, 10% glycerol, 0.5 % Triton X-100, 10 mM β-glycerophosphate, 50 mM NaF, 0.2 mM Na_3VO_4, protease inhibitors (Roche, 11836153001)) using Lysing Matrix C tubes (MP Biomedicals, 6912-100) and the FastPrep-24 (MP Biomedicals) high-speed benchtop homogenizer in the 4 °C room (disrupt worms for 20 seconds at 6.5 m/s, rest on ice for 1 min; repeat twice). Lysed animals were centrifuged at 14,000 rpm for 10 min at 4 °C to pellet worm debris, and supernatant was collected for DARTS. Protein concentration was determined by BCA Protein Assay kit (Pierce, 23223). A worm lysate concentration of 1.13 μg/μL was used for the DARTS experiment. All steps were performed on ice or at 4 °C to help prevent premature protein degradation. TNC buffer (50 mM Tris-HCl pH 8.0, 50 mM NaCl, 10 mM $CaCl_2$) was added to the worm lysates. Worm lysates were incubated with vehicle control (H_2O) or α-KG for 1 h on ice and then 50 min at room temperature. Pronase (Roche, 10165921001) digestions were performed for 30 min at room temperature and stopped by adding SDS loading buffer and heating at 70 °C for 10 min. Samples were then subjected to SDS-PAGE on NuPAGE Novex 4–12% Bis-Tris gradient gels (Invitrogen, NP0322BOX), and Western blotting was carried out with an antibody against ATP5B (Sigma, AV48185) that also recognizes ATP-2.

Complex V activity assay

Complex V activity was assayed using the MitoTox OXPHOS Complex V Activity Kit (Abcam, ab109907). Vehicle (H_2O) or α-KG was mixed with the enzyme prior to the addition of phospholipids. In experiments using octyl α-KG, vehicle (1% DMSO) or octyl α-KG was added with the phospholipids. Relative complex V activity was compared to vehicle. Oligomycin (Sigma, O4876) was used as a positive control for the assay.

Isolation of mitochondria from mouse liver

Animal studies were performed under approved UCLA animal research protocols. Mitochondria from 3-month-old C57BL/6 mice were isolated as described[40]. Briefly, livers were extracted, minced at 4 °C in MSHE+BSA (70 mM sucrose, 210 mM mannitol, 5 mM HEPES, 1 mM EGTA, and 0.5% fatty acid free BSA, pH 7.2), and rinsed several times to remove blood. All subsequent steps were performed on ice or at 4 °C. The tissue was disrupted in 10 volumes of MSHE+BSA with a glass Dounce homogenizer (5–6 strokes) and the homogenate was centrifuged at 800 × *g* for 10 min to remove tissue debris and nuclei. The supernatant was decanted through a cell strainer and centrifuged at 8,000 × *g* for

10 min. The dark mitochondrial pellet was resuspended in MSHE+BSA and re-centrifuged at 8,000 × *g* for 10 min. The final mitochondrial pellets were used for various assays as described below.

Submitochondrial particle (SMP) ATPase assay

ATP hydrolysis by ATP synthase was measured using submitochondrial particles (see[41] and refs therein). Mitochondria were isolated from mouse liver as described above. The final mitochondrial pellet was resuspended in buffer A (250 mM sucrose, 10 mM Tris-HCl, 1 mM ATP, 5 mM $MgCl_2$, and 0.1 mM EGTA, pH 7.4) at 10 μg/μL, subjected to sonication on ice (Fisher Scientific Model 550 Sonic Dismembrator; medium power, alternating between 10 s intervals of sonication and resting on ice for a total of 60 s of sonication), and then centrifuged at 18,000 × *g* for 10 min at 4 °C. The supernatant was collected and centrifuged at 100,000 × *g* for 45 min at 4 °C. The final pellet (submitochondrial particles) was resuspended in buffer B (250 mM sucrose, 10 mM Tris-HCl, and 0.02 mM EGTA, pH 7.4).

The SMP ATPase activity was assayed using the Complex V Activity Buffer as above. The production of ADP is coupled to the oxidation of NADH to NAD^+ through pyruvate kinase and lactate dehydrogenase. The addition of α-KG (up to 10 mM) did not affect the activity of pyruvate kinase or lactate dehydrogenase when external ADP was added. The absorbance decrease of NADH at 340 nm correlates to ATPase activity. SMPs (2.18 ng/uL) were incubated with vehicle or α-KG for 90 min at room temperature prior to the addition of activity buffer, and then the absorbance decrease of NADH at 340 nm was measured every 1 min for 1 h. Oligomycin (Cell signaling, 9996) was used as a positive control for the assay.

Assay for ATP levels

Normal human diploid fibroblast WI-38 (ATCC, CCL-75) cells were seeded in 96-well plates at 2×10^4 cells per well. Cells were treated with either DMSO (vehicle control) or octyl α-KG at varying concentrations for 2 h in triplicate. ATP levels were measured using the CellTiter-Glo luminescent ATP assay (Promega, G7572); luminescence was read using Analyst HT (Molecular Devices). In parallel, identically treated cells were lysed in M-PER (Thermo Scientific, 78501) to obtain protein concentration by BCA Protein Assay kit (Pierce, 23223). ATP levels were normalized to protein content. Statistical analysis was performed using GraphPad Prism (unpaired *t*-test).

Assay for ATP levels in *C. elegans*. Synchronized day 1 adult wildtype *C. elegans* were placed on NGM plates containing either vehicle or 8 mM α-KG. On day 2 and 8 of adulthood, 9 replicates and 4 replicates, respectively, of about 100 worms were collected from α-KG or vehicle control plates, washed 4 times in M9 buffer, and frozen in −80 °C. Animals were lysed using Lysing Matrix C tubes (MP Biomedicals, 6912-100) and the FastPrep-24 (MP Biomedicals) high-speed benchtop homogenizer (disrupt worms for 20 s at 6.5 m/s, rest on ice for 1 min; repeat twice). Lysed animals were centrifuged at 14,000 rpm for 10 min at 4 °C to pellet worm debris, and supernatant was saved for ATP quantitation using the Kinase-Glo Luminescent Kinase Assay Platform (Promega, V6713) according to manufacturer's instructions. Assay was performed in white opaque 96 well tissue culture

plates (Falcon, 353296), and luminescence was measured using Analyst HT (Molecular Devices). ATP levels were normalized to number of worms. Statistical analysis was performed using Microsoft Excel (*t*-test, two-tailed, two-sample unequal variance).

Measurement of oxygen consumption rates (OCR)

OCR measurements were made using a Seahorse XF-24 analyzer (Seahorse Bioscience)[42]. Cells were seeded in Seahorse XF-24 cell culture microplates at 50,000 cells/well in DMEM media supplemented with 10% FBS and 10 mM glucose, and incubated at 37 °C and 5% CO_2 for overnight. Treatment with octyl α-KG or DMSO (vehicle control) was for 1 h. Cells were washed in unbuffered DMEM medium (pH 7.4, 10 mM glucose) just prior to measurement, and maintained in this buffer with indicated concentrations of octyl α-KG. Oxygen consumption rates were measured 3 times under basal conditions and normalized to protein concentration per well. Statistical analysis was performed using GraphPad Prism.

Measurement of oxygen consumption rates (OCR) in living *C. elegans*. Protocol adapted from[43,44]. Wildtype day 1 adult N2 worms were placed on NGM plates containing 8 mM α-KG or H_2O (vehicle control) seeded with OP50 or HT115 *E. coli*. OCR was assessed on day 2 of adulthood. On day 2 of adulthood, worms were collected and washed 4 times with M9 to rid the samples of bacteria (we further verified that α-KG does not affect oxygen consumption of the bacteria – therefore, even if there were any leftover bacteria after the washes, the changes in OCR observed would still be worm-specific), and then the animals were seeded in quadruplicates in Seahorse XF-24 cell culture microplates (Seahorse Bioscience, V7-PS) in 200 μL M9 at ~200 worms per well. Oxygen consumption rates were measured 7 times under basal conditions and normalized to the number of worms counted per well. The experiment was repeated twice. Statistical analysis was performed using Microsoft Excel (*t*-test, two-tailed, two-sample unequal variance).

Measurement of mitochondrial respiratory control ratio (RCR)

Mitochondrial RCR was analyzed using isolated mouse liver mitochondria (see[15] and refs therein). Mitochondria were isolated from mouse liver as described above. The final mitochondrial pellet was resuspended in 30 μL of MAS buffer (70 mM sucrose, 220 mM mannitol, 10 mM KH_2PO_4, 5 mM $MgCl_2$, 2 mM HEPES, 1 mM EGTA, and 0.2% fatty acid free BSA, pH 7.2).

Isolated mitochondrial respiration was measured by running coupling and electron flow assays as described[40]. For the coupling assay, 20 μg of mitochondria in complete MAS buffer (MAS buffer supplemented with 10 mM succinate and 2 μM rotenone) were seeded into a XF24 Seahorse plate by centrifugation at 2,000 × g for 20 min at 4 °C. Just before the assay, the mitochondria were supplemented with complete MAS buffer for a total of 500 μL (with 1% DMSO or octyl α-KG), and warmed at 37 °C for 30 min before starting the oxygen consumption rate measurements. Mitochondrial respiration begins in a coupled State 2; State 3 is initiated by 2 mM ADP; State 4o (oligomycinin-sensitive, i.e., Complex V-independent) is induced by 2.5 μM oligomycin and State 3u (FCCP uncoupled maximal respiratory capacity) by 4 μM FCCP. Finally, 1.5 μg/mL antimycin A was injected at the end of the assay. The State 3/State 4o ratio gives the respiratory control ratio (RCR).

For the electron flow assay, the MAS buffer was supplemented with 10 mM sodium pyruvate (Complex I substrate), 2 mM malate (Complex II inhibitor), and 4 μM FCCP, and the mitochondria are seeded the same way as described for the coupling assay. After basal readings, the sequential injections were as follows: 2 μM rotenone (Complex I inhibitor), 10 mM succinate (Complex II substrate), 4 μM antimycin A (Complex III inhibitor), and 10 mM/100 μM ascorbate/tetramethylphenylenediamine (Complex IV substrate).

ATP synthase enzyme inhibition kinetics

ATP synthesis enzyme inhibition kinetic analysis was performed using isolated mitochondria. Mitochondria were isolated from mouse liver as described above. The final mitochondrial pellet was resuspended in MAS buffer supplemented with 5 mM sodium ascorbate (Sigma, A7631) and 5 mM TMPD (Sigma, T7394).

The reaction was carried out in MAS buffer containing 5 mM sodium ascorbate, 5 mM TMPD, luciferase reagent (Roche, 11699695001), octanol or octyl α-KG, variable amounts of ADP (Sigma, A2754), and 3.75 ng/μL mitochondria. ATP synthesis was monitored by the increase in luminescence over time by a luminometer (Analyst HT, Molecular Devices). ATP synthase-independent ATP formation, derived from the oligomycin-insensitive luminescence, was subtracted as background. The initial velocity of ATP synthesis was calculated from the slope of the first 3 min of the reaction, before the velocity begins to decrease. Enzyme inhibition kinetics was analyzed by nonlinear regression least squares fit using GraphPad Prism.

Assay for mammalian TOR (mTOR) pathway activity

mTOR pathway activity in cells treated with octyl α-KG or oligomycin was determined by the levels of phosphorylation of known mTOR substrates, including S6K (T389), 4E-BP1 (S65), AKT (S473), and ULK1 (S757)[45–49]. Specific antibodies used: P-S6K T389 (Cell Signaling, 9234), S6K (Cell Signaling, 9202S), P-4E-BP1 S65 (Cell Signaling, 9451S), 4E-BP1 (Cell Signaling, 9452S), P-AKT S473 (Cell Signaling, 4060S), AKT (Cell Signaling, 4691S), P-ULK1 S757 (Cell Signaling, 6888), ULK1 (Cell Signaling, 4773S), and GAPDH (Santa Cruz Biotechnology, 25778).

Assay for autophagy

DA2123 animals carrying an integrated GFP::LGG-1 translational fusion gene[50–52], were used to quantify levels of autophagy. To obtain a synchronized population of DA2123, we performed an egg preparation of gravid adults (by lysing ~100 gravid worms in 70 μL M9 buffer, 25 μL bleach and 5 μL 10 N NaOH), and allowed the eggs to hatch overnight in M9 causing starvation induced L1 diapause. L1 larvae were deposited onto NGM treatment plates containing vehicle, 8 mM α-KG, or 40 μM oligomycin, and seeded with either *E. coli* OP50, HT115(DE3) with an empty vector, or HT115(DE3) expressing dsRNAs targeting *atp-2*, *CeTOR/let-363*, or *ogdh-1* as indicated. When the majority of animals in a given sample first reached the mid L3 stage, individual L3 larvae were mounted onto microscope slides and anesthetized with 1.6 mM levamisole (Sigma, 31742). Nematodes were observed using an Axiovert 200M Zeiss confocal microscope with a LSM5 Pascal laser, and images were captured using the LSM Image Examiner (Zeiss). For each specimen, GFP::LGG-1

puncta (autophagosomes) in the epidermis, including the lateral seam cells and Hyp7, were counted in three separate regions of 140.97 μm^2 using *analyze particles* in ImageJ[53]. Measurements were made blind to both the genotype and supplement. Statistical analysis was performed using Microsoft Excel (*t*-test, two-tailed, two-sample unequal variance).

Assay for autophagy in mammalian cells. HEK-293 cells were seeded in 6-well plates at 2.5 × 10^5 cells/well in DMEM media supplemented with 10% FBS and 10 mM glucose, and incubated overnight before treatment with either octanol (vehicle control) or octyl α-KG for 72 h. Cells were lysed in M-PER buffer with protease and phosphatase inhibitors. Lysates were subjected to SDS-PAGE on a 4–12% Bis-Tris gradient gel with MES running buffer and Western blotted for LC3 (Novus, NB100-2220). LC3 is the mammalian homolog of worm LGG-1, and conversion of the soluble LC3-I to the lipidated LC3-II is activated in autophagy, e.g., upon starvation[54].

Pharyngeal pumping rates of *C. elegans* treated with 8 mM α-KG

The pharyngeal pumping rates of 20 wildtype N2 worms per condition were assessed. Pharyngeal contractions were recorded for 1 min using a Zeiss M2BioDiscovery microscope and an attached Sony NDR-XR500V video camera at 12-fold optical zoom. The resulting videos were played back at 0.3× speed using MPlayerX and pharyngeal pumps were counted. Statistical analysis was performed using Microsoft Excel (*t*-test, two-tailed, two-sample unequal variance).

Assay for α-KG levels in *C. elegans*

Synchronized adult worms were collected from plates with vehicle (H_2O) or 8 mM α-KG, washed 3 times with M9 buffer, and flash frozen. Worms were lysed in M9 using Lysing Matrix C tubes (MP Biomedicals, 6912-100) and the FastPrep-24 (MP Biomedicals) high-speed benchtop homogenizer in the 4 °C room (disrupt worms for 20 seconds at 6.5 m/s, rest on ice for 1 min; repeat three times). Lysed animals were centrifuged at 14,000 rpm for 10 min at 4 °C to pellet worm debris, and the supernatant was saved. The protein concentration of the supernatant was determined by the BCA Protein Assay kit (Pierce, 23223); there was no difference in protein level per worm in α-KG treated and vehicle treated animals (data not shown). α-KG content was assessed as described previously[55] with modifications. Worm lysates were incubated at 37 °C in 100 mM KH_2PO_4 (pH 7.2), 10 mM NH_4Cl, 5 mM $MgCl_2$, and 0.3 mM NADH for 10 minutes. Glutamate dehydrogenase (Sigma, G2501) was then added to reach a final concentration of 1.83 units/mL. Under these conditions glutamate dehydrogenase uses α-KG and NADH to make glutamate. The absorbance decrease was monitored at 340 nm. The intracellular level of α-KG was determined from the absorbance decrease in NADH. The approximate molarity of α-KG present inside the animals was estimated using average protein content (~245 ng/worm, from BCA assay) and volume (~3 nL for adult worms 1.1 mm in length and 60 μm in diameter (http://www.wormatlas.org/hermaphrodite/introduction/Introframeset.html)).

For quantitative analysis of α-KG in worms using UHPLC-ESI/MS/MS, synchronized day 1 adult worms were placed on vehicle plates with or without bacteria for 24 h, and then collected and lysed in the same manner as above. α-KG analysis by LC/MS/MS was carried

out on an Agilent 1290 Infinity UHPLC system and 6460 Triple Quadrupole mass spectrometer (Agilent Technologies) using an electrospray ionization (ESI) source with Agilent Jet Stream technology. Data were acquired with Agilent MassHunter Data Acquisition software version B.06.00, and processed for precursor and product ions selection with MassHunter Qualitative Analysis software version B.06.00 and for calibration and quantification with MassHunter Quantitative Analysis for QQQ software version B. 06.00.

For UHPLC, 3 μL calibration standards and samples were injected onto the UHPLC system including a G4220A binary pump with a built-in vacuum degasser and a thermostatted G4226A high performance autosampler. An ACQUITY UPLC BEH Amide analytical column (2.1 × 50 mm, 1.7 μm) and a VanGuard BEH Amide Pre-column (2.1 × 5 mm, 1.7 μm) from Waters Corporation were used at the flow rate of 0.6 mL/min using 50/50/0.04 acetonitrile/water/ammonium hydroxide with 10 mM ammonium acetate as mobile phase A and 95/5/0.04 acetonitrile/water/ammonium hydroxide with 10 mM ammonium acetate as mobile phase B. The column was maintained at room temperature. The following gradient was applied: 0–0.41 min: 100% B isocratic; 0.41–5.30 min: 100–30% B; 5.3–5.35 min: 30-0% B; 5.35–7.35 min: 0% B isocratic; 7.35–7.55 min: 0–100%B; 7.55–9.55 min: 100% B isocratic.

For the MS detection, the ESI mass spectra data were recorded on a negative ionization mode by MRM. MRM transitions of α-KG and its ISTD $^{13}C_4$-α-KG (Cambridge Isotope Laboratories) were determined using a 1-min 37% B isocratic UHPLC method through the column at flow rate of 0.6 mL/min. The precursor ion of $[M-H]^-$ and the product ion of $[M-CO_2-H]^-$ were observed to have the highest signal to noise ratios. The precursor and product ions are respectively 145.0 and 100.9 for AKG, and 149.0 and 104.9 for ISTD $^{13}C_4$-α-KG. Nitrogen was used as the drying, sheath, and collision gas. All the source and analyzer parameters were optimized using Agilent MassHunter Source and iFunnel Optimizer and Optimizer software respectively. The source parameters are as follows: drying gas temperature 120 °C, drying gas flow 13 L/min, nebulizer pressure 55 psi, sheath gas temperature 400 °C, sheath gas flow 12 L/min, capillary voltage 2000 V, and nozzle voltage 0 V. The analyzer parameters are as follows: fragmentor voltage 55 V, collision energy 2 V, and cell accelerator voltage 1 V. The UHPLC eluants before 1 min and after 5.3 min were diverted to waste.

Membrane-permeable esters of α-KG

Octyl α-KG, a commonly used membrane-permeable ester of α-KG[55–58], was used to deliver α-KG across lipid membranes in experiments using cells and mitochondria. Upon hydrolysis by cellular esterases, octyl α-KG yields α-KG and the byproduct octanol. We showed that, whereas octanol control has no effect (Extended Data Fig. 2e–f and Extended Data Fig. 6a), α-KG alone can bind and inhibit ATP synthase (Fig. 2a–b, Extended Data Fig. 2a–b, and data not shown), decrease ATP and OCR (Fig. 2e, and Fig. 2g), induce autophagy (Fig. 4b), and increase *C. elegans* lifespan (Fig. 1, Fig. 3, and Extended Data Figs. 1, 5, and Table 2). The existence and activity of esterases in our mitochondrial and cell culture experiments have been confirmed using calcein AM (C1430, Molecular Probes), an

esterase substrate that fluoresces upon hydrolysis, and also by mass spectrometry (data not shown). The hydrolysis by esterases explains why distinct esters of α-KG, such as 1-octyl α-KG, 5-octyl α-KG, and dimethyl α-KG, have similar effects to α-KG (Extended Data Fig. 2g–h and Extended Data Table 2).

Synthesis of octyl α-KG—Synthesis of 1-octyl α-KG has been published by GD and MEJ[59]. Briefly, 1-octanol (0.95 mL, 6.0 mmol), DMAP (37 mg, 0.3 mmol), and DCC (0.743 g, 3.6 mmol) were added to a solution of 1-cyclobutene-1-carboxylic acid (0.295 g, 3.0 mmol) in dry CH_2Cl_2 (6.0 mL) at 0 °C. After it had stirred for 1 h, the solution was allowed to warm to room temperature and stirred for another 8 h. The precipitate was filtered and washed with ethyl acetate (3 × 100 mL). The combined organic phases were washed with water and brine, and dried over anhydrous Na_2SO_4. Flash column chromatography on silica gel eluting with 80/1 hexane/ethyl acetate gave octyl cyclobut-1-enecarboxylate as a clear oil (0.604 g, 96%). To a −78 °C solution of this oil (0.211 g, 1.0 mmol) in CH_2Cl_2 (10 mL) was bubbled O_3/O_2 until the solution turned blue. The residual ozone was discharged by bubbling with O_2 and the reaction was warmed to room temperature and stirred for another 1 h. Dimethyl sulfide (Me_2S, 0.11 mL, 1.5 mmol) was added to the mixture and it was stirred for another 2 h. The CH_2Cl_2 was removed in vacuo and the crude product was dissolved in a solution of 2-methyl-2-butene (0.8 mL) in *t*-BuOH (3.0 mL). To this was added dropwise a solution containing sodium chlorite (0.147 g, 1.3 mmol) and sodium dihydrogen phosphate monohydrate (0.179 g, 1.3 mmol) in H_2O (1.0 mL). The mixture was stirred at room temperature overnight, and then extracted with ethyl acetate (3 × 50 mL). The combined organic phases were washed with water and brine, and dried over anhydrous Na_2SO_4. Flash column chromatography on silica gel eluting with 5/1 hexane/ethyl acetate gave octyl α-KG which became a pale solid when stored in the refrigerator (0.216 g, 84%).

Synthesis of 5-octyl L-Glu ((*S*)-2-amino-5-(octyloxy)-5-oxopentanoic acid)—L-Glutamic acid (0.147 g, 1.0 mmol) and anhydrous sodium sulfate (0.1 g) was dissolved in octanol (2.0 mL), and then tetrafluoroboric acid-dimethyl ether complex (0.17 mL) was added. The suspended mixture was stirred at 21 °C overnight. Anhydrous THF (5 mL) was added to the mixture and it was filtered through a thick pad of activated charcoal. Anhydrous triethylamine (0.4 mL) was added to the clear filtrate to obtain a milky white slurry. Upon trituration with ethyl acetate (10 mL), the monoester monoacid precipitated. The precipitate was collected, washed with additional ethyl acetate (2 × 5 mL), and dried in vacuo to give the desired product 5-octyl L-Glu (0.249 g, 96%) as a white solid. ^{1}H NMR (500 MHz, Acetic acid-d_4): δ 4.12 (dd, *J* = 6.6, 6.6 Hz, 1H), 4.11 (t, *J* = 6.8 Hz, 2H), 2.64 (m, 2H), 2.26 (m, 2H), 1.64 (m, 2H), 1.30 (m, 10H), 0.89 (t, *J* = 7.0 Hz, 3H). ^{13}C NMR (125 MHz, Acetic acid-d_4): 175.0, 174.3, 66.3, 55.0, 32.7, 30.9, 30.11, 30.08, 29.3, 26.7, 26.3, 23.4, 14.4.

Synthesis of 5-octyl D-Glu ((*R*)-2-amino-5-(octyloxy)-5-oxopentanoic acid)—The synthesis of the opposite enantiomer, i.e., 5-octyl D-Glu, was carried out by the exact same procedure starting with D-glutamic acid. The spectroscopic data was identical to that of the enantiomeric compound.

Synthesis of 5-octyl α-KG (5-(Octyloxy)-2,5-dioxopentanoic acid) 1-Benzyl 5-octyl 2-oxopentanedioate—To a solution of 5-octyl L-Glu (0.249 g) in H_2O (6.0 mL) and acetic acid (2.0 mL) cooled to 0 °C was added slowly a solution of aqueous sodium nitrite (0.207 g, 3.0 mmol in 4 mL H_2O). The reaction mixture was allowed to warm slowly to room temperature and was stirred overnight. The mixture was concentrated. The resulting residue was dissolved in DMF (10 mL) and $NaHCO_3$ (0.42 g, 5.0 mmol) and benzyl bromide (0.242 mL, 2.0 mmol) were added to the mixture. The mixture was stirred at 21 °C overnight and then extracted with ethyl acetate (3 × 30 mL). The combined organic phase was washed with water and brine and dried over anhydrous $MgSO_4$. Flash column chromatography on silica gel eluting with 7/1 hexanes/ethyl acetate gave the mixed diester 1-benzyl 5-octyl (*S*)-2-hydroxypentanedioate as a colorless oil. To this oil dissolved in dichloromethane (10.0 mL), were added $NaHCO_3$ (0.42 g, 5.0 mmol) and Dess-Martin periodinane (0.509 g, 1.2 mmol) and the mixture was stirred at room temperature for 1 h and then extracted with ethyl acetate (3 × 30 mL). The combined organic phase was washed with water and brine and dried over anhydrous $MgSO_4$. Flash column chromatography on silica gel eluting with 5/1 hexanes/ethyl acetate gave the desired 1-benzyl 5-octyl 2-oxopentanedioate (0.22 g, 66%) as a white solid. ^{1}H NMR (500 MHz, $CDCl_3$): 7.38 (m, 5H), 5.27 (s, 2H), 4.05 (t, *J* = 6.5 Hz, 2H), 3.14 (t, *J* = 6.5 Hz, 2H), 2.64 (t, *J* = 6.5 Hz, 2H), 1.59 (m, 2H), 1.28 (m, 10H), 0.87 (t, *J* = 7.0 Hz, 3H). ^{13}C NMR (125 MHz, $CDCl_3$): 192.2, 171.9, 160.1, 134.3, 128.7, 128.6, 128.5, 67.9, 65.0, 34.2, 31.7, 29.07, 29.05, 28.4, 27.5, 25.7, 22.5, 14.0.

5-octyl α-KG (5-(Octyloxy)-2,5-dioxopentanoic acid)—To a solution of 1-benzyl 5-octyl 2-oxopentanedioate (0.12 g, 0.344 mmol) in ethyl acetate (15 mL) was added 5% Pd/C (80 mg). Over the mixture was passed a stream of argon and then the argon was replaced with hydrogen gas and the mixture was stirred vigorously for 15 min. The mixture was filtered through a thick pad of Celite to give the desired product 5-octyl α-KG (0.088 g, 99%) as white solid. ^{1}H NMR (500 MHz, $CDCl_3$): 8.16 (br s, 1H), 4.06 (t, *J* = 6.5 Hz, 2H), 3.18 (t, *J* = 6.5 Hz, 2H), 2.69 (t, *J* = 6.0 Hz, 2H), 1.59 (m, 2H), 1.26 (m, 10H), 0.85 (t, *J* = 7.0 Hz, 3H). ^{13}C NMR (125 MHz, $CDCl_3$): 193.8, 172.7, 160.5, 65.5, 33.0, 31.7, 29.08, 29.06, 28.4, 27.8, 25.8, 22.5, 14.0.

Extended Data

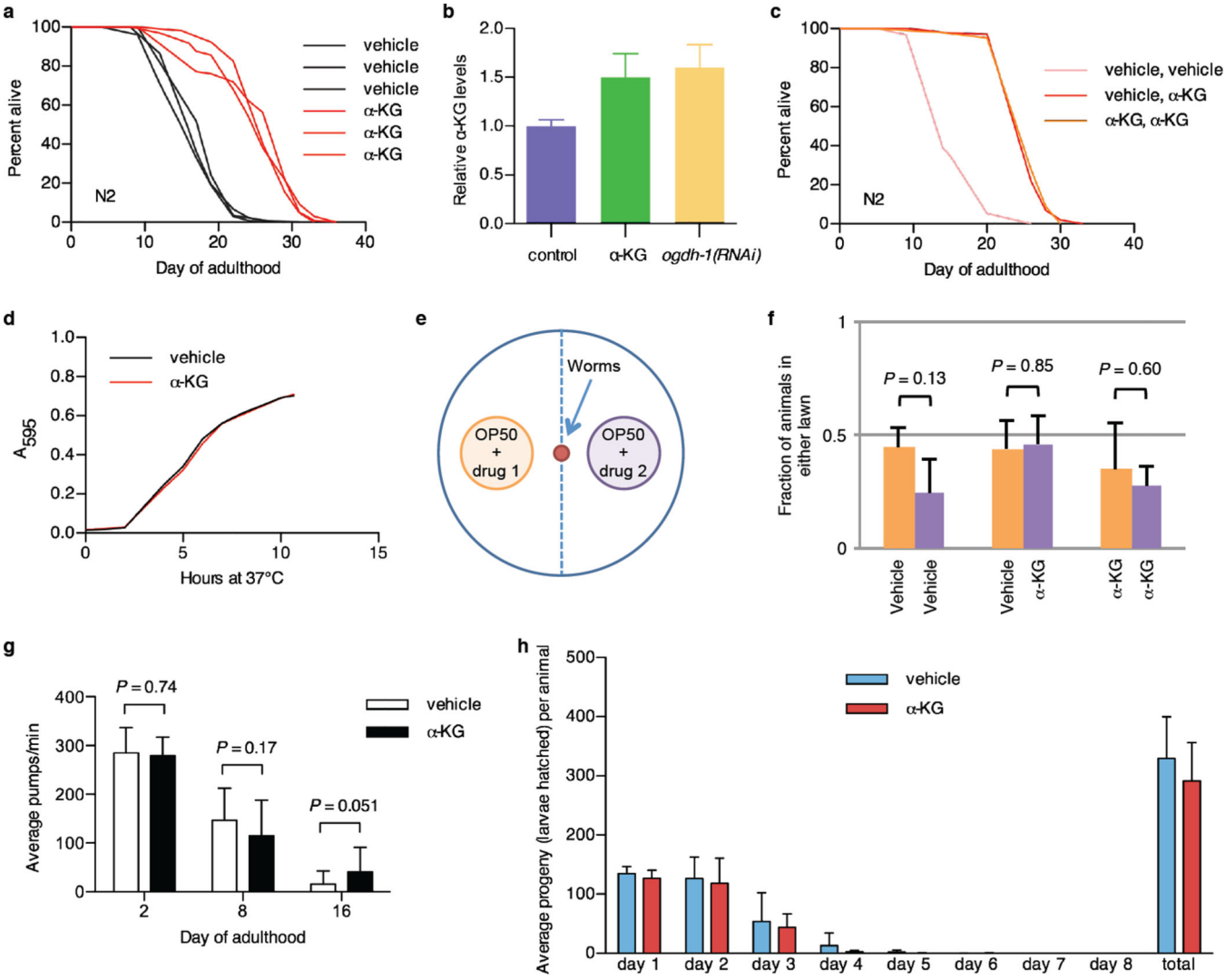

Extended Data Figure 1.

a, Robust lifespan extension in adult *C. elegans* by α-KG. 8 mM α-KG increased the mean lifespan of N2 by an average of 47.3% in three independent experiments ($P < 0.0001$ for every experiment, by log-rank test). Expt. #1, $m_{veh} = 18.9$ ($n = 87$), $m_{\alpha\text{-KG}} = 25.8$ ($n = 96$); Expt. #2, $m_{veh} = 17.5$ ($n = 119$), $m_{\alpha\text{-KG}} = 25.4$ ($n = 97$); Expt. #3, $m_{veh} = 16.3$ ($n = 100$), $m_{\alpha\text{-KG}} = 26.1$ ($n = 104$). *m*, mean lifespan (days of adulthood); *n*, number of animals tested. **b**, Worms supplemented with 8 mM α-KG and worms with RNAi knockdown of α-KGDH (encoded by *ogdh-1*) have increased α-KG levels. Young adult worms were placed on treatment plates seeded with control HT115 *E. coli* or HT115 expressing *ogdh-1* dsRNA, and α-KG content was assayed after 24 h (see Methods). **c**, α-KG treatment beginning at the egg stage and that beginning in adulthood produced identical lifespan increases. Light red, treatment with vehicle control throughout larval and adult stages ($m = 15.6$, $n = 95$); dark red, treatment with vehicle during larval stages and with 8 mM α-KG at adulthood ($m = 26.3$, $n = 102$), $P < 0.0001$ (log-rank test); orange, treatment with 8 mM α-KG throughout

larval and adult stages (m = 26.3, n = 102), $P < 0.0001$ (log-rank test). m, mean lifespan (days of adulthood); n, number of animals tested. **d**, α-KG does not alter the growth rate of the OP50 *E. coli*, which is the standard laboratory food source for nematodes. α-KG (8 mM) or vehicle (H_2O) was added to standard LB media and the pH was adjusted to 6.6 by the addition of NaOH. Bacterial cells from the same overnight OP50 culture were added to the LB ± α-KG mixture at a 1:40 dilution, and then placed in the 37 °C incubator shaker at 300 rpm. The absorbance at 595 nm was read at 1 h time intervals to generate the growth curve. **e**, Schematic representation of food preference assay. **f**, N2 worms show no preference between OP50 *E. coli* food treated with vehicle or α-KG (P = 0.85, by t-test, two-tailed, two-sample unequal variance), nor preference between identically treated OP50 *E. coli*. **g**, Pharyngeal pumping rate of *C. elegans* on 8 mM α-KG is not significantly altered (by t-test, two-tailed, two-sample unequal variance). **h**, Brood size of *C. elegans* treated with 8 mM α-KG. Brood size analysis was conducted at 20 °C. 10 L4 wildtype worms were each singly placed onto an NGM plate containing vehicle or 8 mM α-KG. Worms were transferred one per plate onto a new plate every day, and the eggs laid were allowed to hatch and develop on the previous plate. Hatchlings were counted as a vacuum was used to remove them from the plate. Animals on 8 mM α-KG showed no significant difference in brood size compared with animals on vehicle plates (P = 0.223, by t-test, two-tailed, two-sample unequal variance). Mean ± s.d is plotted in all cases.

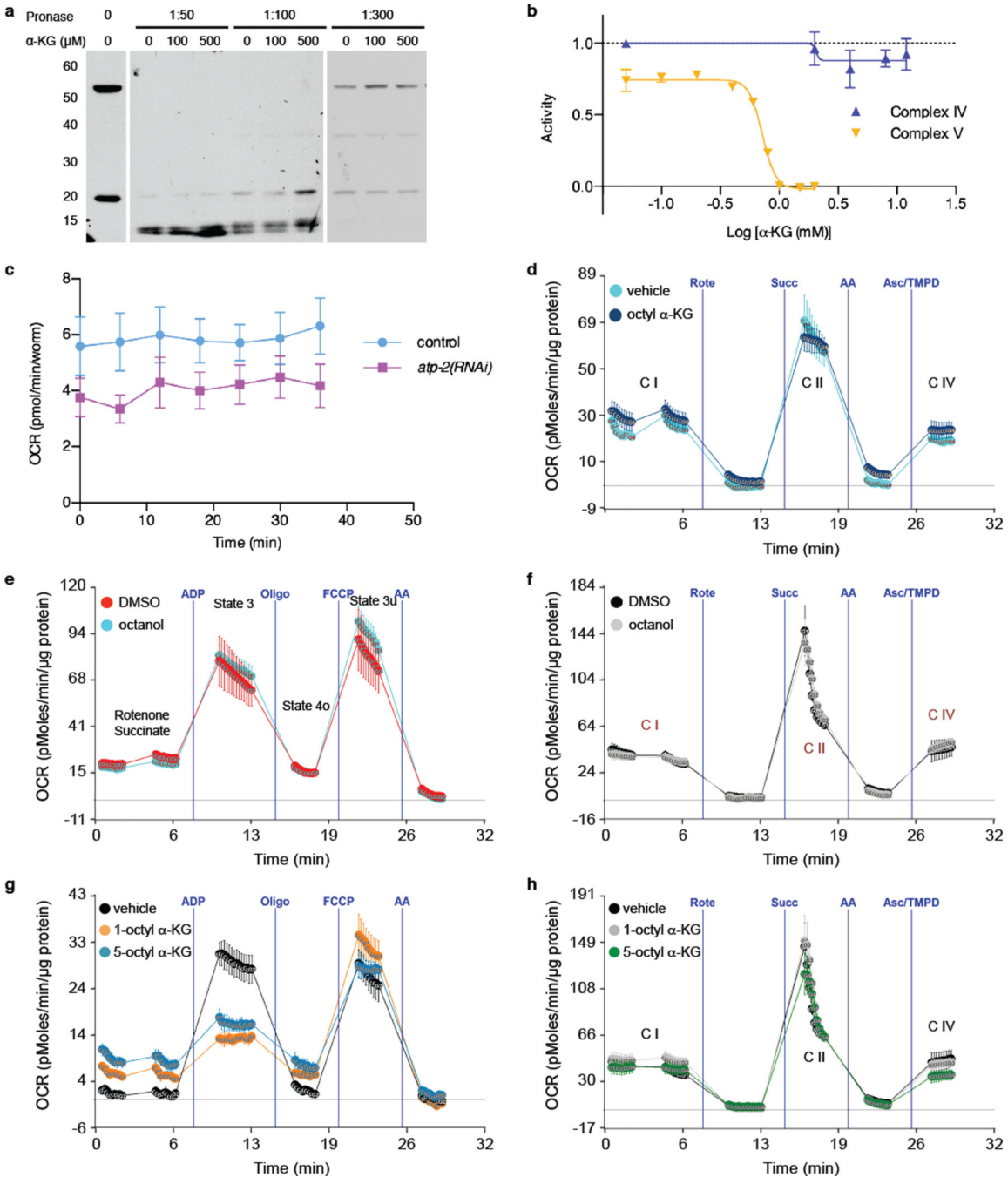

Extended Data Figure 2.

a, Western blot showing protection of the ATP-2 protein from Pronase digestion upon α-KG binding in the DARTS assay. The antibody for human ATP5B (Sigma, AV48185) recognizes the epitope $_{144}$IMNVIGEPIDERGPIKTKQFAPIHAEAPEFMEMSVEQEILVTGIKVVDLL$_{193}$ that has 90% identity to the *C. elegans* ATP-2. The lower molecular weight band near 20 kDa is a proteolytic fragment of the full-length protein corresponding to the domain directly bound by α-KG. **b**, α-KG does not affect Complex IV activity. Complex IV activity was

assayed using the MitoTox OXPHOS Complex IV Activity Kit (Abcam, ab109906). Relative complex IV activity was compared to vehicle (H_2O) controls. Potassium cyanide (Sigma, 60178) was used as a positive control for the assay. Complex V activity was assayed using the MitoTox Complex V OXPHOS Activity Microplate Assay (Abcam, ab109907). **c**, *atp-2(RNAi)* worms have lower oxygen consumption compared to control (*gfp* in RNAi vector), $P < 0.0001$ (*t*-test, two-tailed, two-sample unequal variance) for the entire time series (2 independent experiments); similar to α-KG treated worms shown in figure 2g. **d**, α-KG does not affect the electron flow through the electron transport chain. OCR from isolated mouse liver mitochondria at basal (pyruvate and malate as Complex I substrate and Complex II inhibitor, respectively, in presence of FCCP) and in response to sequential injection of rotenone (Rote; Complex I inhibitor), succinate (Succ; Complex II substrate), antimycin A (AA; complex III inhibitor), ascorbate / tetramethylphenylenediamine (Asc/TMPD; cytochrome c (Complex IV) substrate). No difference in Complex I (C I), Complex II (C II), or Complex IV (C IV) respiration was observed after 30 min treatment with 800 μM of octyl α-KG, whereas Complex V was inhibited (see Fig. 2h) by the same treatment (2 independent experiments). **e-f**, No significant difference in coupling (**e**) or electron flow (**f**) was observed with either octanol or DMSO vehicle control. **g-h**, Treatment with 1-octyl α-KG or 5-octyl α-KG gave identical results in coupling (**g**) or electron flow (**h**) assays. Mean ± s.d. is plotted in all cases.

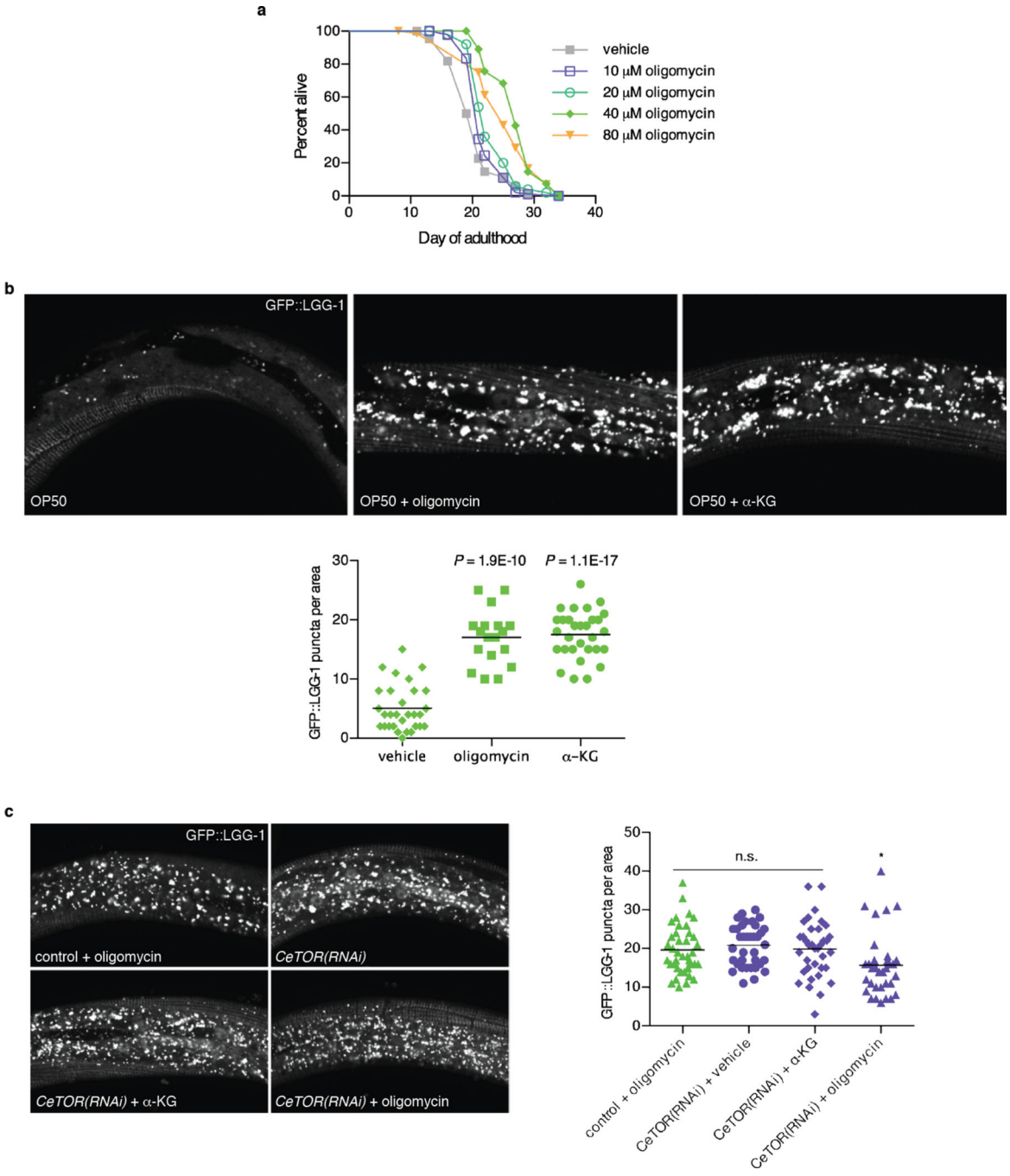

Extended Data Figure 3.

a, Oligomycin extends the lifespan of adult *C. elegans* in a concentration dependent manner. Treatment with oligomycin began at the young adult stage. 40 μM oligomycin increased the mean lifespan of N2 worms by 32.3% ($P < 0.0001$, by log-rank test); see Extended Data Table 2 for details. **b**, Confocal images of GFP::LGG-1 puncta in L3 epidermis of *C. elegans* with vehicle, oligomycin (40 μM), or α-KG (8 mM), and number of GFP::LGG-1 containing puncta quantitated using ImageJ. Bars indicate the mean. Autophagy in *C. elegans* treated with oligomycin or α-KG is significantly higher than in vehicle-treated

control animals (*t*-test, two-tailed, two-sample unequal variance). **c**, There is no significant difference (n.s.) between control worms treated with oligomycin and *CeTOR(RNAi)* worms treated with vehicle, nor between vehicle and α-KG treated *CeTOR(RNAi)* worms, consistent with independent experiments in Fig. 4b-c; also, oligomycin does not augment autophagy in *CeTOR(RNAi)* worms (if anything, there may be a small decrease*); by *t*-test, two-tailed, twosample unequal variance. Bars indicate the mean.

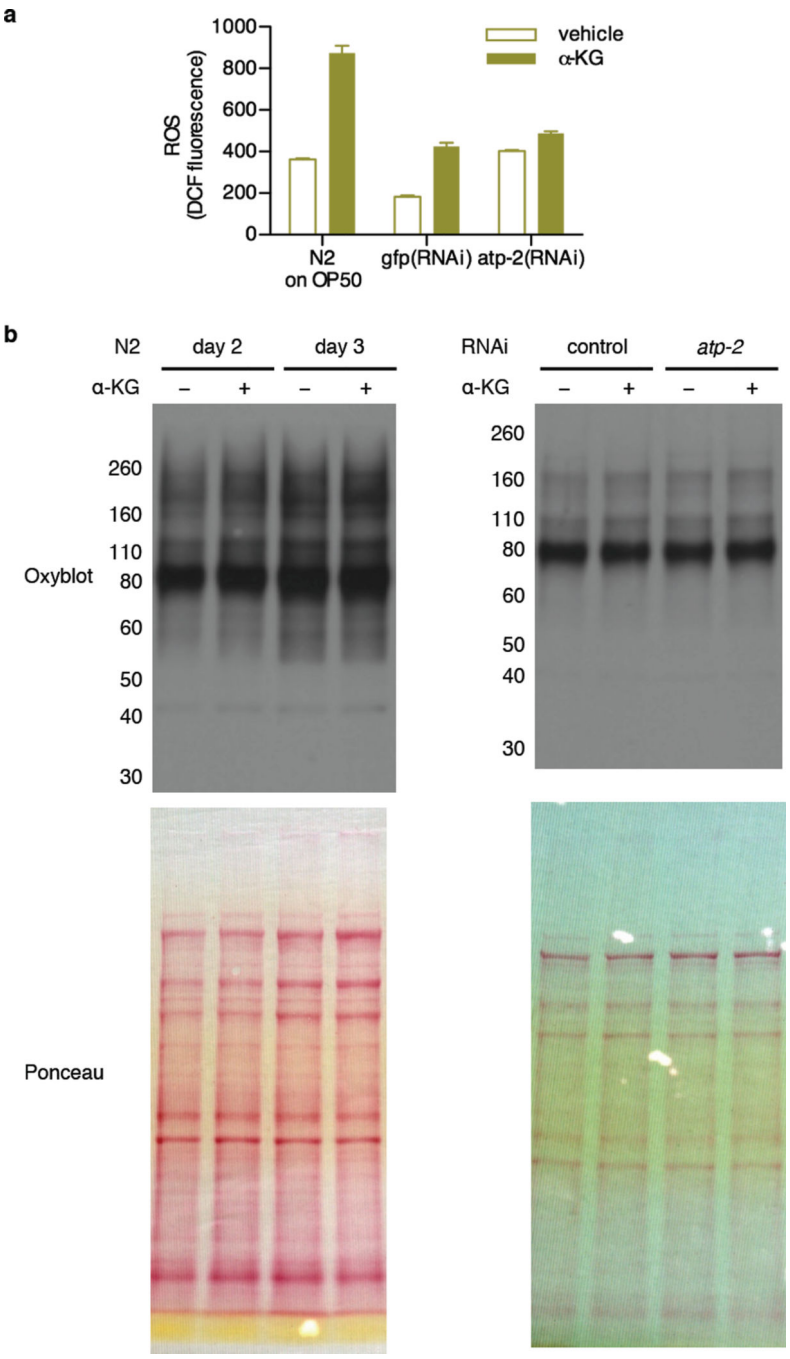

Extended Data Figure 4.

a, The *atp*-2*(RNAi)* worms have higher levels of DCF fluorescence than *gfp* control worms ($P < 0.0001$, by *t*-test, two-tailed, two-sample unequal variance). Supplementation with α-KG also leads to higher DCF fluorescence, in both HT115 (for RNAi) and OP50 fed worms ($P = 0.0007$, and $P = 0.0012$, respectively). ROS levels were measured using 2',7'-dichlorodihydrofluorescein diacetate (H_2DCF-DA). Since whole worm lysates were used, total cellular oxidative stress was measured here. H_2DCF-DA (Molecular Probes, D399) was dissolved in ethanol to a stock concentration of 1.5 mg/mL. Fresh stock was prepared every time prior to use. For measuring ROS in worm lysates, a working concentration of H_2DCF-DA at 30 ng/mL was hydrolyzed by 0.1 M NaOH at room temperature for 30 min to generate 2', 7'-dichlorodihydrofluorescein (DCFH) before mixing with whole worm lysates in a black 96-well plate (Greiner Bio-One). Oxidation of DCFH by ROS yields the highly fluorescent 2', 7'-dichlorofluorescein (DCF). DCF fluorescence was read at excitation / emission of 485 / 530 nm using SpectraMax MS (Molecular Devices). H_2O_2 was used as positive control (not shown). To prepare the worm lysates, synchronized young adult animals were cultivated on plates containing vehicle or 8 mM α-KG and OP50 or HT115 *E. coli* for 1 day, and then collected and lysed as described in "Assay for ATP levels in *C. elegans*" (see Methods). Mean ± s.d. is plotted. **b**, There was no significant change in protein oxidation upon α-KG treatment or *atp-2(RNAi)*. Oxidized protein levels were determined by the OxyBlot. Synchronized young adult N2 animals were placed onto plates containing vehicle or 8 mM α-KG, and seeded with OP50 or HT115 bacteria that expressed control or *atp-2* dsRNA. Adult day 2 and day 3 worms were collected and washed 4 times with M9 buffer, and then stored at −80 °C for at least 24 h. Laemmli buffer (Biorad, 161-0737) was added to every sample and animals were lysed by alternate boil/freeze cycles. Lysed animals were centrifuged at 14,000 rpm for 10 min at 4 °C to pellet worm debris, and supernatant was collected for oxyblot analysis. Protein concentration of samples was determined by the 660 nm Protein Assay (Thermo Scientific, 1861426) and normalized for all samples. Carbonylation of proteins in each sample was detected using the OxyBlot Protein Oxidation Detection Kit (Millipore, S7150).

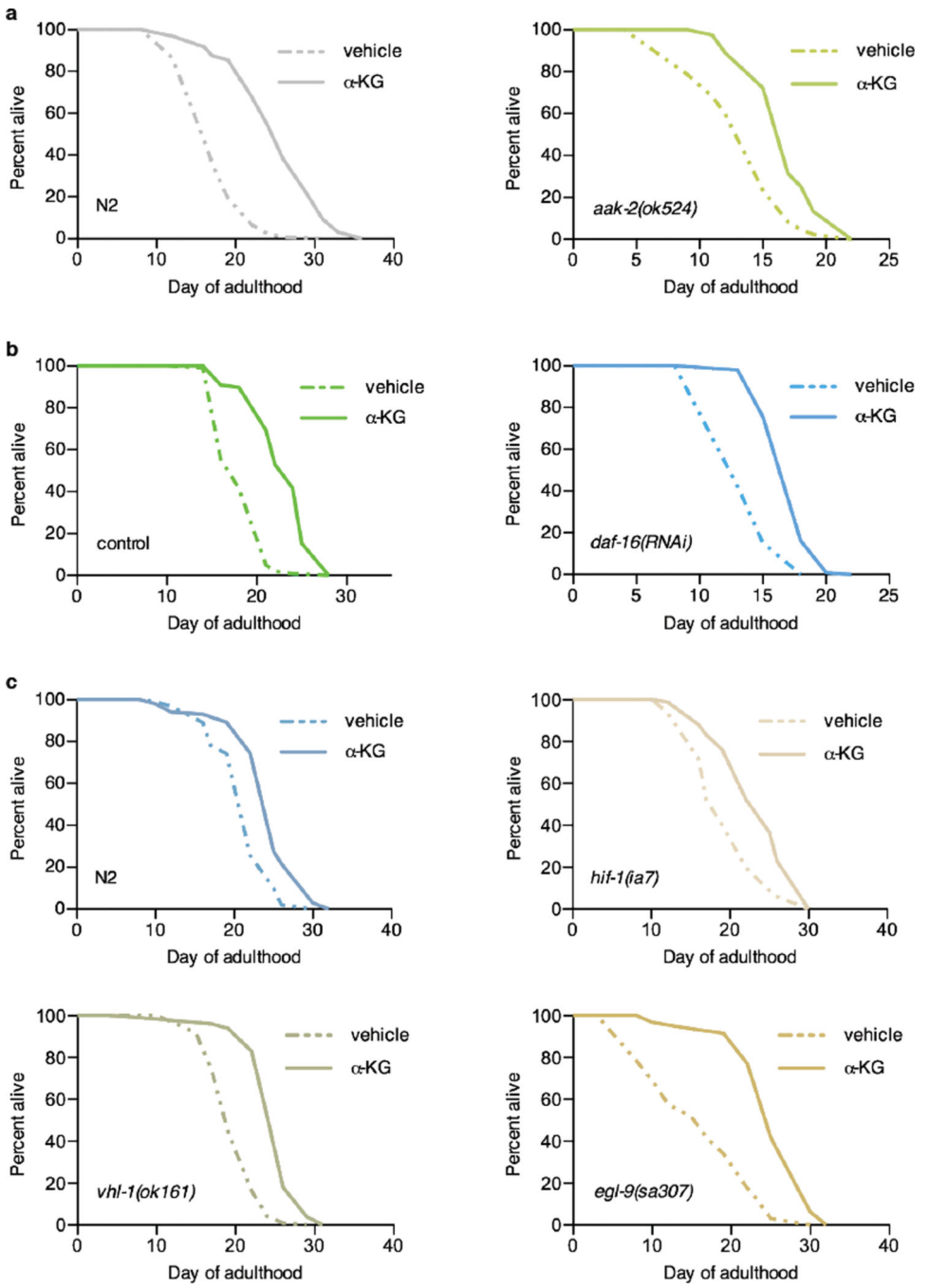

Extended Data Figure 5.

Lifespans of α-KG supplemented **a**, N2 worms, m_{veh} = 17.5 (n = 119), $m_{\alpha\text{-KG}}$ = 25.4 (n = 97), $P < 0.0001$; or *aak-2(ok524)* mutants, m_{veh} = 13.7 (n = 85), $m_{\alpha\text{-KG}}$ = 17.1 (n = 83), $P < 0.0001$. **b**, N2 worms fed *gfp* RNAi control, m_{veh} = 18.5 (n = 101), $m_{\alpha\text{-KG}}$ = 23.1 (n = 98), $P < 0.0001$; or *daf-16* RNAi, m_{veh} = 14.3 (n = 99), $m_{\alpha\text{-KG}}$ = 17.6 (n = 99), $P < 0.0001$. **c**, N2 worms, m_{veh} = 21.5 (n = 101), $m_{\alpha\text{-KG}}$ = 24.6 (n = 102), $P < 0.0001$; *hif-1(ia7)* mutants, m_{veh} = 19.6 (n = 102), $m_{\alpha\text{-KG}}$ = 23.6 (n = 101), $P < 0.0001$; *vhl-1(ok161)* mutants, m_{veh} = 20.0 (n = 98), $m_{\alpha\text{-KG}}$ = 24.9 (n = 100), $P < 0.0001$; or *egl-9(sa307)* mutants, m_{veh} = 16.2 (n = 97),

$m_{\alpha\text{-KG}}$ = 25.6 (n = 96), $P < 0.0001$. m, mean lifespan (days of adulthood); n, number of animals tested. P-values were determined by the log-rank test. Number of independent experiments: *N2* (8), *hif-1* (5), *vhl-1* (1), and *egl-9* (2); see Extended Data Table 2 for details. Two different *hif-1* mutant alleles 27 have been used: *ia4* (shown in Fig. 3g) is a deletion over several introns and exons; *ia7* (shown above) is an early stop codon, causing a truncated protein. Both alleles have the same effect on lifespan 27. We tested both alleles for α-KG longevity and obtained the same results.

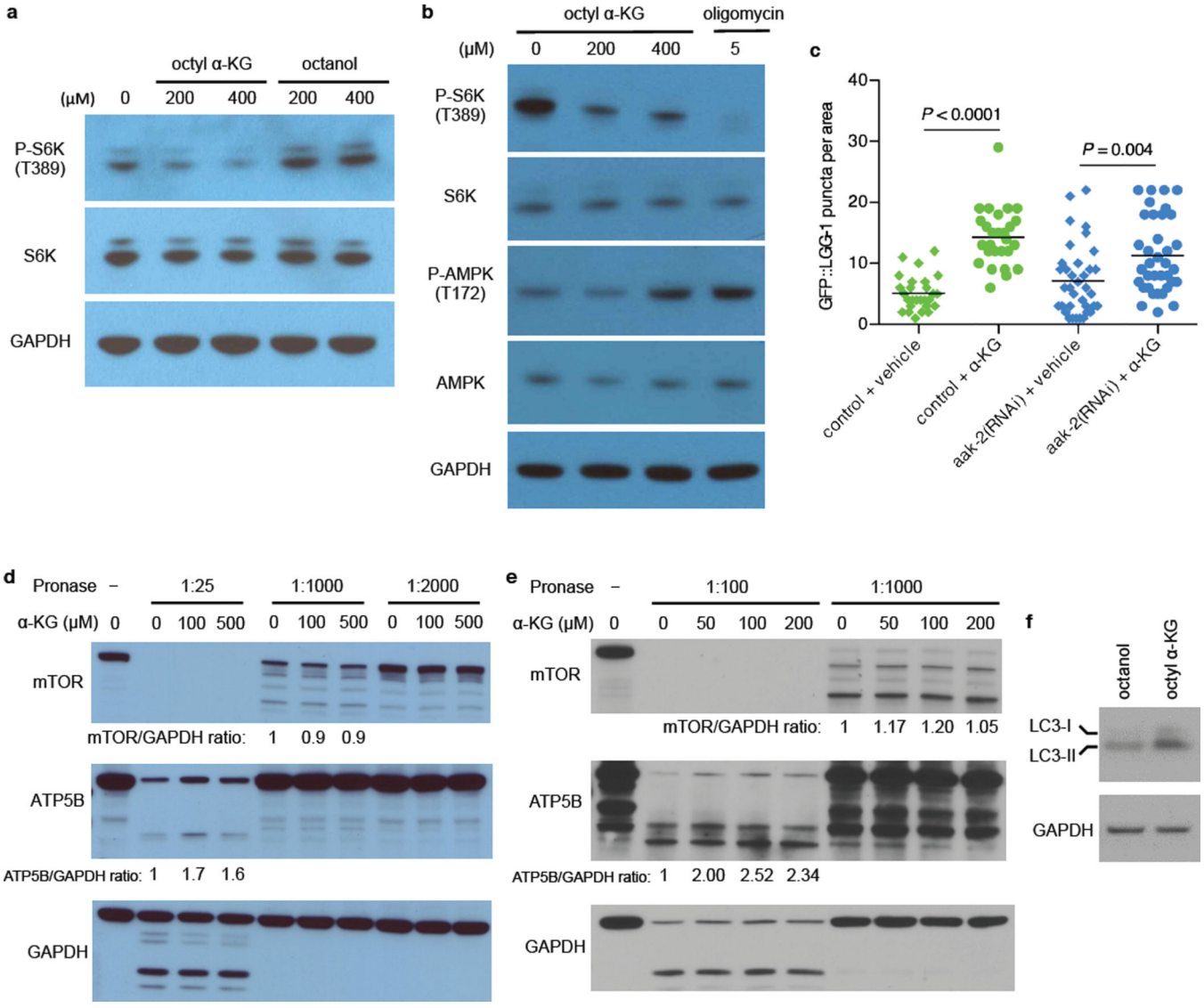

Extended Data Figure 6.

a, Phosphorylation of S6K (T389) was decreased in U87 cells treated with octyl α-KG, but not in cells treated with octanol control. Same results were obtained using HEK-293 and MEF cells. **b**, Phosphorylation of AMPK (T172) is upregulated in WI-38 cells upon Complex V inhibition by α-KG, consistent with decreased ATP content in α-KG treated cells and animals. However, this activation of AMPK appears to require more severe

Complex V inhibition than the inactivation of mTOR, as either oligomycin or a higher concentration of octyl α-KG was required for increasing P-AMPK whereas concentrations of octyl α-KG comparable to those that decreased cellular ATP content (Fig. 2d) or oxygen consumption (Fig. 2f) were also sufficient for decreasing P-S6K. Same results were obtained using U87 cells. Western blotted with specific antibodies against P-AMPK T172 (Cell Signaling, 2535S) and AMPK (Cell Signaling, 2603S). **c**, α-KG still induces autophagy in *aak-2(RNAi)* worms; $^{**}P < 0.01$ (*t*-test, two-tailed, two-sample unequal variance). Number of GFP::LGG-1 containing puncta was quantitated using ImageJ. Bars indicate the mean. **d-e**, α-KG does not bind to TOR directly as determined by DARTS. HEK-293 (**d**) or HeLa (**e**) cells were lysed in M-PER buffer (Thermo Scientific, 78501) with the addition of protease inhibitors (Roche, 11836153001) and phosphatase inhibitors (50 mM NaF, 10 mM β-glycerophosphate, 5 mM sodium pyrophosphate, 2 mM Na_3VO_4). Protein concentration of the lysate was measured by BCA Protein Assay kit (Pierce, 23227). Chilled TNC buffer (50 mM Tris-HCl pH 8.0, 50 mM NaCl, 10 mM $CaCl_2$) was added to the protein lysate, and the protein lysate was then incubated with vehicle control (DMSO) or varying concentrations of α-KG for 1 h (for **d**) or 3 h (for **e**) at room temperature. Pronase (Roche, 10165921001) digestions were performed for 20 min at room temperature, and stopped by adding SDS loading buffer and immediately heating at 95 °C for 5 min (for **d**) or 70 °C for 10 min (for **e**). Samples were subjected to SDS-PAGE on 4–12% Bis-Tris gradient gel (Invitrogen, NP0322BOX) and Western blotted with specific antibodies against ATP5B (Santa Cruz, sc58618), mTOR (Cell Signaling, 2972), or GAPDH (Ambion, AM4300). ImageJ was used to quantify the mTOR/GAPDH and ATP5B/GAPDH ratios. Susceptibility of the mTOR protein to Pronase digestion is unchanged in the presence of α-KG, whereas, as expected, Pronase resistance in the presence of α-KG is increased for ATP5B, which we identified as a new binding target of α-KG. **f**, Increased autophagy in HEK-293 cells treated with octyl α-KG was confirmed by Western blot analysis of MAP1 LC3 (Novus, NB100-2220), consistent with decreased phosphorylation of the autophagy initiating kinase ULK1 (Fig. 4a).

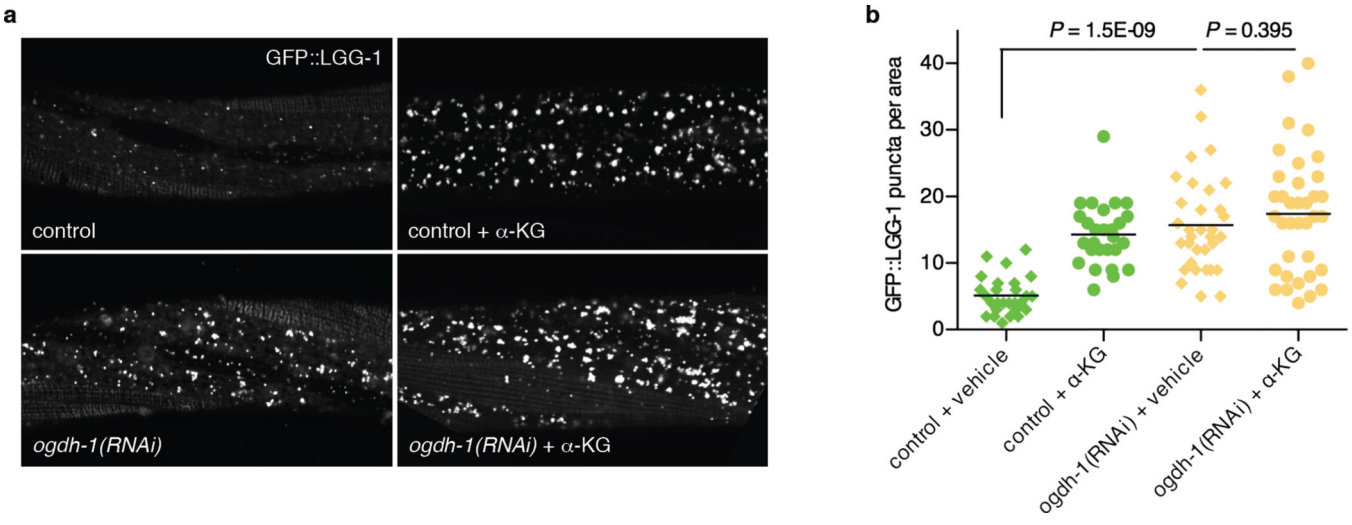

Extended Data Figure 7.

a, Confocal images of GFP::LGG-1 puncta in the epidermis of mid L3 stage, control or *ogdh-1* knockdown, *C. elegans* treated with vehicle or α-KG (8 mM). **b**, Number of GFP::LGG-1 puncta quantitated using ImageJ. Bars indicate the mean. *ogdh-1(RNAi)* worms have significantly higher autophagy levels, and α-KG does not significantly augment autophagy in *ogdh-1(RNAi)* worms (*t*-test, two-tailed, two-sample unequal variance).

Extended Data Table 1

Enriched proteins in the α-KG DARTS sample.

Protein Symbol	Protein Name	Score	Control sample		α-KG sample		Enrichment
			Spectra	Peptides	Spectra	Peptides	
ATP5B	ATP synthase subunit beta	4088	23	9	121	15	5.3
HSPD1	60 kDa heat shock protein	2352	31	11	138	29	4.5
PKM2	Pyruvate kinase isozymes M1/M2	2203			56	7	
LCP1	Plastin-2	1865	14	8	76	13	5.4
ATP5A1	ATP synthase subunit alpha	1616	41	9	61	12	1.5
SHMT2	Serine hydroxymethyltransferase	1060	7	5	33	10	4.7
HSP90AA1	Heat shock protein HSP 90-alpha	952	29	8	44	8	1.5
EEF2	Elongation factor 2	943	4	2	37	9	9.3
DDX5	Probable ATP-dependent RNA helicase DDX5	652	7	3	33	10	4.7
HSPA8	Heat shock cognate 71 kDa protein	615	4	2	35	10	8.8

Only showing those proteins with at least 15 spectra in α-KG sample and enriched at least 1.5 fold.

Extended Data Table 2

Summary of lifespan data

Strain	*m* (mean lifespan, days)		% difference	*p*-value	*n* (number of animals)	
	vehicle	α-KG			vehicle	α-KG
N2	18.9	25.8	36.3	< 0.0001	87	96
N2	17.5	25.4	45.6	< 0.0001	119	97
N2	16.3	26.1	60.2	< 0.0001	100	104
eat-2(ad1116)	22.8	22.9	0.5	0.79	59	40
daf-16(mu86)	16.3	18.8	15.1	< 0.0001	106	105
eat-2(ad1116)	21.1	24.0	13.4	0.23	39	59
daf-2(e1370)	38.0	47.6	25.1	< 0.0001	72	69
N2	13.2	22.3	69.8	< 0.0001	100	104
daf-16(mu86)	13.4	17.4	29.5	< 0.0001	71	72
daf-16(RNAi)	14.3	17.6	22.9	< 0.0001	99	99
N2	16.1	19.1	19.3	0.0003	97	96
daf-2(e1370)	38.3	43.9	14.6	< 0.0001	109	101
aak-2(ok524)	13.7	17.1	24.3	< 0.0001	85	83
aak-2(ok524)	16.4	17.5	6.7	< 0.0001	97	97

Strain	*m* (mean lifespan, days)		% difference	*p*-value	*n* (number of animals)	
	vehicle	α-KG			vehicle	α-KG
aak-2(RNAi)	16.2	19.9	23.3	< 0.0001	93	92
N2	15.6	26.3	68.8	< 0.0001	95	102
N2	15.6	26.3	68.5	< 0.0001	95	102
egl-9(sa307)	16.2	25.6	58.6	< 0.0001	97	96
egl-9(sa307)	19.5	27.3	40.3	< 0.0001	95	101
N2	14.7	21.6	46.9	< 0.0001	100	88
N2	14.0	20.7	47.9	< 0.0001	112	114
N2	21.5	24.6	14.6	< 0.0001	101	102
hif-1(ia4)	20.5	26.0	26.5	< 0.0001	85	71
hif-1(ia7)	19.6	23.6	20.4	< 0.0001	102	101
hif-1(ia4)	21.5	24.7	14.7	< 0.0001	88	87
N2	16.7	23.4	39.7	< 0.0001	104	103
N2	15.8	22.2	40.5	< 0.0001	104	94
N2	18.4	24.6	33.4	< 0.0001	99	89
vhl-1(ok161)	20.0	25.0	24.9	< 0.0001	98	100
hif-1(ia7)	12.4	17.3	38.9	< 0.0001	97	90
hif-1(ia7)	17.9	23.7	32.0	< 0.0001	58	55
N2	16.8	22.4	32.7	< 0.0001	104	101
N2	15.7	21.6	37.6	< 0.0001	85	99
smg-1(cc546ts)	18.4	23.8	29.5	< 0.0001	110	87
smg-1(cc546ts);pha-4(zu225)	14.2	13.5	−4.9	0.5482	94	109
smg-1(cc546ts);pha-4(zu225)	17.6	15.2	−14.0	0.0877	28	34
N2	13.6	20.7	51.8	< 0.0001	103	104
smg-1(cc546ts)	16.2	23.0	42.2	< 0.0001	114	121
smg-1(cc546ts);pha-4(zu225)	13.8	15.2	10.2	0.254	45	45
EV RNAi control	18.6	23.4	26.1	< 0.0001	94	91
atp-2(RNAi)	22.8	22.5	−1.3	0.3471	97	94
EV RNAi control	18.8	22.7	20.6	< 0.0001	97	94
gfp RNAi control	18.5	23.1	25.3	< 0.0001	101	98
α-kgdh(RNAi)	21.2	21.1	−0.7	0.65	98	100
CeTOR(RNAi)	22.1	23.6	6.8	0.02	94	95
gfp RNAi control	20.2	27.7	37.4	< 0.0001	99	81
CeTOR(RNAi)	25.1	25.7	2.1	0.9511	96	74
EV RNAi control	22.8	27.2	21.6	<0.0001	70	72
CeTOR(RNAi)	27.4	27.2	−0.8	0.7239	64	80
EV RNAi control	19.7	24.3	23.8	< 0.0001	93	84
atp-2(RNAi)	25.3	23.4	−7.4	< 0.0001	87	63

Strain	*m*		% difference	*p-value*	*n*		[oligomycin]
	vehicle	oligomycin			vehicle	oligomycin	

Strain	*m* (mean lifespan, days)		% difference	*p*-value	*n* (number of animals)		
	vehicle	α-KG			vehicle	α-KG	
N2	20.4	25.5	25.2	< 0.0001	88	72	80 μM
N2		27.0	32.3	< 0.0001		82	40 μM
N2		23.1	13.2	0.0005		50	20 μM
N2		22.0	7.9	0.0106		90	10 μM

Strain	*m*		% difference	*p-value*	*n*		treatment
	vehicle	treatment			vehicle	treatment	
N2	14.5	16.9	16.8	0.0005	73	71	octyl α-KG (500 μM)
N2	14.5	17.0	16.8	< 0.0001	73	60	α-KG
N2	14.0	18.8	33.9	< 0.0001	112	114	dimethyl α-KG
N2	14.0	20.7	47.8	< 0.0001	112	114	α-KG
N2	15.7	21.6	37.6	< 0.0001	85	99	disodium α-KG

Strain	*m*		% difference	*p-value*	*n*		food source
	vehicle	α-KG			vehicle	α-KG	
N2	17.4	21.2	21.6	0.0001	108	55	live OP50
N2	19.0	23.0	21.0	0.0003	88	46	dead OP50 (γ-irradiated)

Acknowledgments

We thank S. Lee, M. Hansen, B. Lemire, A. van der Bliek, S. Clarke, T. K. Blackwell, R. Johnson, J. E. Walker, A. G. W. Leslie, K. N. Houk, B. Martin, J. Lusis, J. Gober, Y. Wang, H. Sun, and anonymous referees for advice and discussions; J. Avruch for CeTOR RNAi vector; J. Powell-Coffman for strains and advice; and K. Yan for technical assistance. Worm strains were provided by the *Caenorhabditis* Genetics Center (CGC), which is funded by NIH Office of Research Infrastructure Programs (P40 OD010440). We thank the U.S. National Institutes of Health for traineeship support of R.M.C. (T32 GM007104), M.Y.P. (T32 GM007185), B.L. (T32 GM008496), and M.N. (T32 CA009120). X.F. is a recipient of the China Scholarship Council Scholarship. G.C.M. was supported by Ford Foundation and National Science Foundation Graduate Research Fellowships.

References

1. Colman RJ, et al. Caloric restriction delays disease onset and mortality in rhesus monkeys. Science. 2009; 325:201–204. [PubMed: 19590001]
2. Mattison JA, et al. Impact of caloric restriction on health and survival in rhesus monkeys from the NIA study. Nature. 2012; 489:318–321. [PubMed: 22932268]
3. Kenyon CJ. The genetics of ageing. Nature. 2010; 464:504–512. [PubMed: 20336132]
4. Harrison DE, et al. Rapamycin fed late in life extends lifespan in genetically heterogeneous mice. Nature. 2009; 460:392–395. [PubMed: 19587680]
5. Williams DS, Cash A, Hamadani L, Diemer T. Oxaloacetate supplementation increases lifespan in Caenorhabditis elegans through an AMPK/FOXO-dependent pathway. Aging Cell. 2009; 8:765–768. [PubMed: 19793063]
6. Lucanic M, et al. N-acylethanolamine signalling mediates the effect of diet on lifespan in Caenorhabditis elegans. Nature. 2011; 473:226–229. [PubMed: 21562563]
7. Lomenick B, et al. Target identification using drug affinity responsive target stability (DARTS). Proc Natl Acad Sci U S A. 2009; 106:21984–21989. [PubMed: 19995983]

8. Abrahams JP, Leslie AG, Lutter R, Walker JE. Structure at 2.8 A resolution of F1-ATPase from bovine heart mitochondria. Nature. 1994; 370:621–628. [PubMed: 8065448]
9. Boyer PD. The ATP synthase--a splendid molecular machine. Annu Rev Biochem. 1997; 66:717–749. [PubMed: 9242922]
10. Tsang WY, Sayles LC, Grad LI, Pilgrim DB, Lemire BD. Mitochondrial respiratory chain deficiency in Caenorhabditis elegans results in developmental arrest and increased life span. J Biol Chem. 2001; 276:32240–32246. [PubMed: 11410594]
11. Dillin A, et al. Rates of behavior and aging specified by mitochondrial function during development. Science. 2002; 298:2398–2401. [PubMed: 12471266]
12. Lee SS, et al. A systematic RNAi screen identifies a critical role for mitochondria in C. elegans longevity. Nat Genet. 2003; 33:40–48. [PubMed: 12447374]
13. Curran SP, Ruvkun G. Lifespan regulation by evolutionarily conserved genes essential for viability. PLoS Genet. 2007; 3:e56. [PubMed: 17411345]
14. Gems D, Riddle DL. Genetic, behavioral and environmental determinants of male longevity in Caenorhabditis elegans. Genetics. 2000; 154:1597–1610. [PubMed: 10747056]
15. Brand MD, Nicholls DG. Assessing mitochondrial dysfunction in cells. Biochem J. 2011; 435:297–312. [PubMed: 21726199]
16. Lakowski B, Hekimi S. The genetics of caloric restriction in Caenorhabditis elegans. Proc Natl Acad Sci U S A. 1998; 95:13091–13096. [PubMed: 9789046]
17. Hansen M, et al. Lifespan extension by conditions that inhibit translation in Caenorhabditis elegans. Aging Cell. 2007; 6:95–110. [PubMed: 17266679]
18. Stanfel MN, Shamieh LS, Kaeberlein M, Kennedy BK. The TOR pathway comes of age. Biochim Biophys Acta. 2009; 1790:1067–1074. [PubMed: 19539012]
19. Hardie DG, Scott JW, Pan DA, Hudson ER. Management of cellular energy by the AMP-activated protein kinase system. FEBS Lett. 2003; 546:113–120. [PubMed: 12829246]
20. Greer EL, Brunet A. Different dietary restriction regimens extend lifespan by both independent and overlapping genetic pathways in C. elegans. Aging Cell. 2009; 8:113–127. [PubMed: 19239417]
21. Sheaffer KL, Updike DL, Mango SE. The Target of Rapamycin pathway antagonizes pha-4/FoxA to control development and aging. Curr Biol. 2008; 18:1355–1364. [PubMed: 18804378]
22. Panowski SH, Wolff S, Aguilaniu H, Durieux J, Dillin A. PHA-4/Foxa mediates diet-restriction-induced longevity of C. elegans. Nature. 2007; 447:550–555. [PubMed: 17476212]
23. Wullschleger S, Loewith R, Hall MN. TOR signaling in growth and metabolism. Cell. 2006; 124:471–484. [PubMed: 16469695]
24. Melendez A, et al. Autophagy genes are essential for dauer development and life-span extension in C. elegans. Science. 2003; 301:1387–1391. [PubMed: 12958363]
25. Loenarz C, Schofield CJ. Expanding chemical biology of 2-oxoglutarate oxygenases. Nat Chem Biol. 2008; 4:152–156. [PubMed: 18277970]
26. Epstein AC, et al. C. elegans EGL-9 and mammalian homologs define a family of dioxygenases that regulate HIF by prolyl hydroxylation. Cell. 2001; 107:43–54. [PubMed: 11595184]
27. Zhang Y, Shao Z, Zhai Z, Shen C, Powell-Coffman JA. The HIF-1 hypoxia-inducible factor modulates lifespan in C. elegans. PLoS One. 2009; 4:e6348. [PubMed: 19633713]
28. Brauer MJ, et al. Conservation of the metabolomic response to starvation across two divergent microbes. Proc Natl Acad Sci U S A. 2006; 103:19302–19307. [PubMed: 17159141]
29. Kaminsky YG, Kosenko EA, Kondrashova MN. Metabolites of citric acid cycle, carbohydrate and phosphorus metabolism, and related reactions, redox and phosphorylating states of hepatic tissue, liver mitochondria and cytosol of the pigeon, under normal feeding and natural nocturnal fasting conditions. Comp Biochem Physiol B. 1982; 73:957–963. [PubMed: 7151427]
30. Brugnara L, et al. Metabolomics approach for analyzing the effects of exercise in subjects with type 1 diabetes mellitus. PLoS One. 2012; 7:e40600. [PubMed: 22792382]
31. Brenner S. The genetics of Caenorhabditis elegans. Genetics. 1974; 77:71–94. [PubMed: 4366476]
32. Timmons L, Fire A. Specific interference by ingested dsRNA. Nature. 1998; 395:854. [PubMed: 9804418]

33. Long X, et al. TOR deficiency in C. elegans causes developmental arrest and intestinal atrophy by inhibition of mRNA translation. Curr Biol. 2002; 12:1448–1461. [PubMed: 12225660]
34. Sutphin GL, Kaeberlein M. Measuring Caenorhabditis elegans life span on solid media. J Vis Exp. 2009
35. Gaudet J, Mango SE. Regulation of organogenesis by the Caenorhabditis elegans FoxA protein PHA-4. Science. 2002; 295:821–825. [PubMed: 11823633]
36. Abada EA, et al. C. elegans behavior of preference choice on bacterial food. Mol Cells. 2009; 28:209–213. [PubMed: 19756391]
37. Lomenick B, Jung G, Wohlschlegel JA, Huang J. Target identification using drug affinity responsive target stability (DARTS). Curr Protoc Chem Biol. 2011; 3:163–180. [PubMed: 22229126]
38. Lomenick B, Olsen RW, Huang J. Identification of direct protein targets of small molecules. ACS Chem Biol. 2011; 6:34–46. [PubMed: 21077692]
39. Stubbs CJ, et al. Application of a proteolysis/mass spectrometry method for investigating the effects of inhibitors on hydroxylase structure. J Med Chem. 2009; 52:2799–2805. [PubMed: 19364117]
40. Rogers GW, et al. High throughput microplate respiratory measurements using minimal quantities of isolated mitochondria. PLoS One. 2011; 6:e21746. [PubMed: 21799747]
41. Alberts, B. Molecular biology of the cell. 3rd edn. Garland Pub.; 1994.
42. Wu M, et al. Multiparameter metabolic analysis reveals a close link between attenuated mitochondrial bioenergetic function and enhanced glycolysis dependency in human tumor cells. Am J Physiol Cell Physiol. 2007; 292:C125–C136. [PubMed: 16971499]
43. Yamamoto H, et al. NCoR1 is a conserved physiological modulator of muscle mass and oxidative function. Cell. 2011; 147:827–839. [PubMed: 22078881]
44. Pathare PP, Lin A, Bornfeldt KE, Taubert S, Van Gilst MR. Coordinate regulation of lipid metabolism by novel nuclear receptor partnerships. PLoS Genet. 2012; 8:e1002645. [PubMed: 22511885]
45. Pullen N, Thomas G. The modular phosphorylation and activation of p70s6k. FEBS Lett. 1997; 410:78–82. [PubMed: 9247127]
46. Burnett PE, Barrow RK, Cohen NA, Snyder SH, Sabatini DM. RAFT1 phosphorylation of the translational regulators p70 S6 kinase and 4E-BP1. Proc Natl Acad Sci U S A. 1998; 95:1432–1437. [PubMed: 9465032]
47. Gingras AC, et al. Hierarchical phosphorylation of the translation inhibitor 4E-BP1. Genes Dev. 2001; 15:2852–2864. [PubMed: 11691836]
48. Sarbassov DD, Guertin DA, Ali SM, Sabatini DM. Phosphorylation and regulation of Akt/PKB by the rictor-mTOR complex. Science. 2005; 307:1098–1101. [PubMed: 15718470]
49. Kim J, Kundu M, Viollet B, Guan KL. AMPK and mTOR regulate autophagy through direct phosphorylation of Ulk1. Nat Cell Biol. 2011; 13:132–141. [PubMed: 21258367]
50. Kang C, You YJ, Avery L. Dual roles of autophagy in the survival of Caenorhabditis elegans during starvation. Genes Dev. 2007; 21:2161–2171. [PubMed: 17785524]
51. Hansen M, et al. A role for autophagy in the extension of lifespan by dietary restriction in C. elegans. PLoS Genet. 2008; 4:e24. [PubMed: 18282106]
52. Alberti A, Michelet X, Djeddi A, Legouis R. The autophagosomal protein LGG-2 acts synergistically with LGG-1 in dauer formation and longevity in C. elegans. Autophagy. 2010; 6:622–633. [PubMed: 20523114]
53. Schneider CA, Rasband WS, Eliceiri KW. NIH Image to ImageJ: 25 years of image analysis. Nat Methods. 2012; 9:671–675. [PubMed: 22930834]
54. Kabeya Y, et al. LC3, a mammalian homologue of yeast Apg8p, is localized in autophagosome membranes after processing. EMBO J. 2000; 19:5720–5728. [PubMed: 11060023]
55. MacKenzie ED, et al. Cell-permeating alpha-ketoglutarate derivatives alleviate pseudohypoxia in succinate dehydrogenase-deficient cells. Mol Cell Biol. 2007; 27:3282–3289. [PubMed: 17325041]

56. Zhao S, et al. Glioma-derived mutations in IDH1 dominantly inhibit IDH1 catalytic activity and induce HIF-1alpha. Science. 2009; 324:261–265. [PubMed: 19359588]

57. Xu W, et al. Oncometabolite 2-hydroxyglutarate is a competitive inhibitor of alpha-ketoglutarate-dependent dioxygenases. Cancer Cell. 2011; 19:17–30. [PubMed: 21251613]

58. Jin G, et al. Disruption of wild-type IDH1 suppresses D-2-hydroxyglutarate production in IDH1-mutated gliomas. Cancer Res. 2013; 73:496–501. [PubMed: 23204232]

59. Jung ME, Deng G. Synthesis of the 1-monoester of 2-ketoalkanedioic acids, for example, octyl alpha-ketoglutarate. J Org Chem. 2012; 77:11002–11005. [PubMed: 23163977]

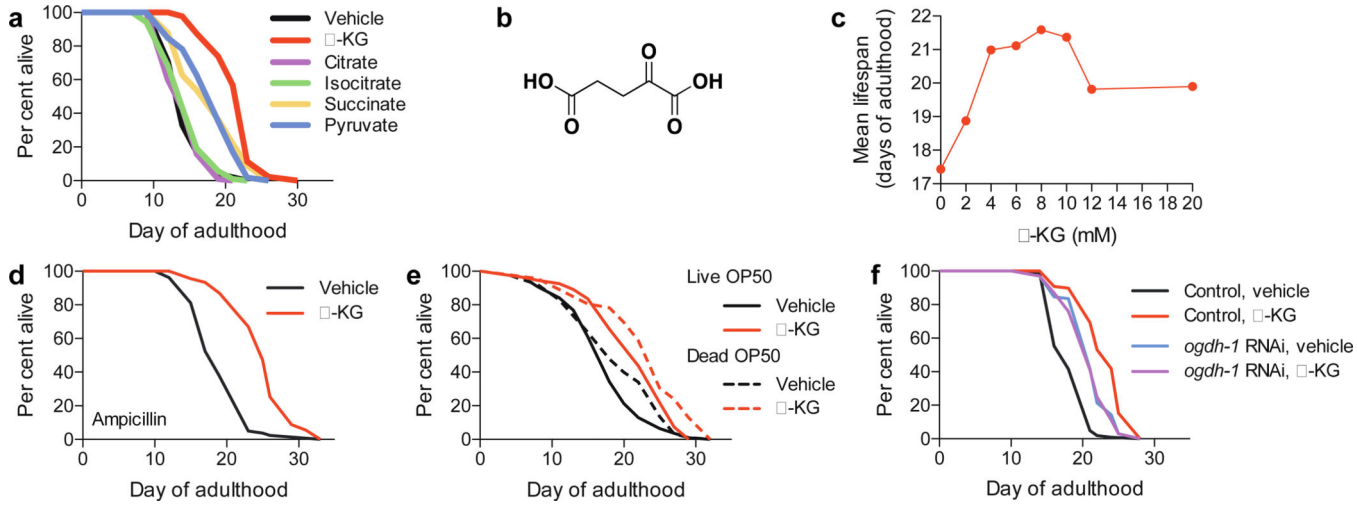

Figure 1. α-KG extends the adult lifespan of *C. elegans*

a, α-KG extends the lifespan of adult worms in the metabolite longevity screen. 8 mM was used for all metabolites. **b**, Structure of α-KG. **c**, Dose response of α-KG in longevity. **d–e**, α-KG extends the lifespan of worms fed bacteria that have been **d**, ampicillin-arrested, m_{veh} = 19.4 (n = 80), $m_{\alpha\text{-KG}}$ = 25.1 (n = 91), $P < 0.0001$ (log-rank test); or **e**, γ-irradiation-killed, m_{veh} = 19.0 (n = 88), $m_{\alpha\text{-KG}}$ = 23.0 (n = 46), $P < 0.0001$ (log-rank test). **f**, α-KG does not further extend the lifespan of *ogdh-1(RNAi)* worms, m_{veh} = 21.2 (n = 98), $m_{\alpha\text{-KG}}$ = 21.1 (n = 100), P = 0.65 (log-rank test). *m*, mean lifespan (days of adulthood); *n*, number of animals tested.

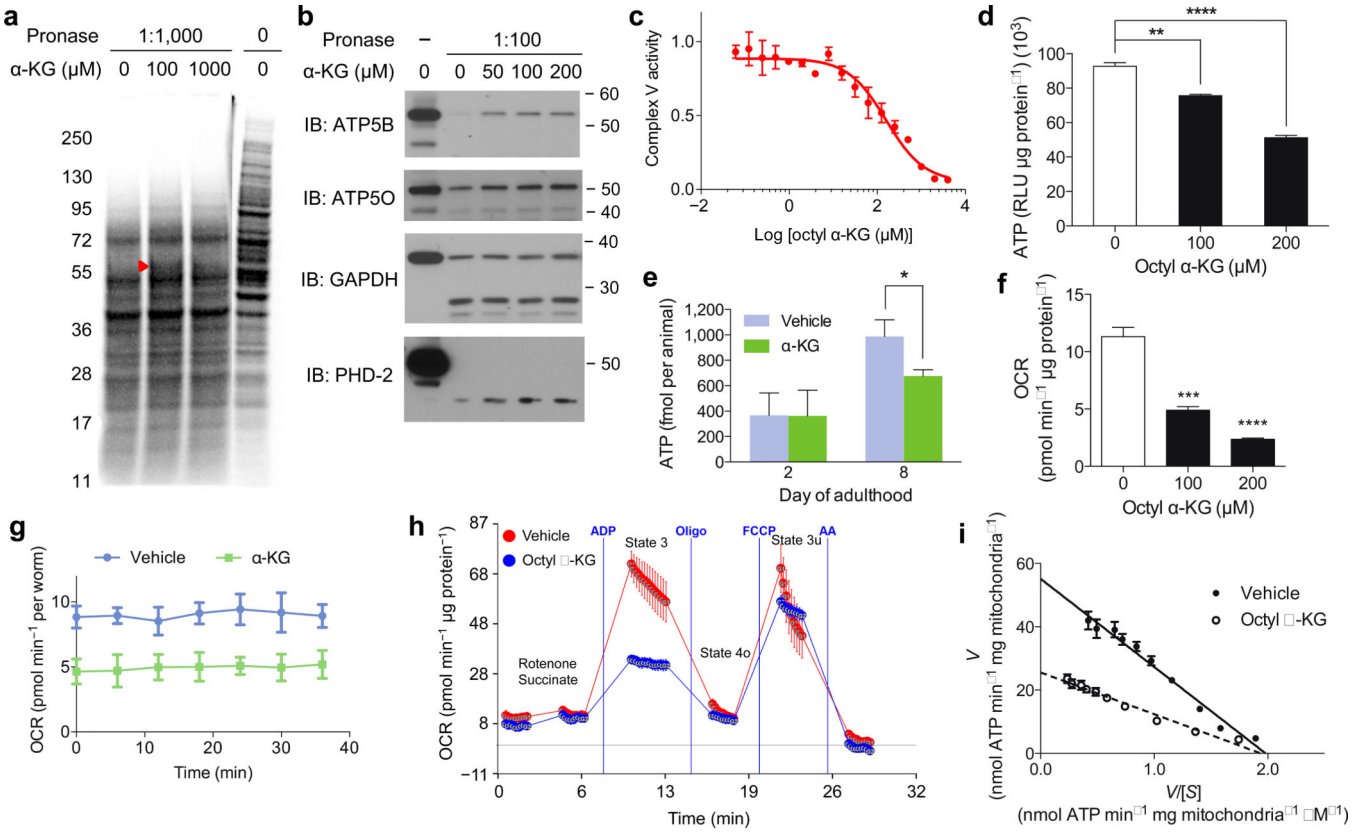

Figure 2. α-KG binds and inhibits ATP synthase

a, DARTS identifies ATP5B as an α-KG-binding protein. Red arrowhead, protected band. **b**, DARTS confirms α-KG binding specifically to ATP5B. **c**, Inhibition of ATP synthase by α-KG (released from octyl α-KG; Supplementary Notes). This inhibition was reversible (not shown). **d–g**, Reduced ATP levels in (**d**) octyl α-KG treated normal human fibroblasts (***P* = 0.0016, *****P* < 0.0001; by *t*-test, two-tailed, two-sample unequal variance) and (**e**) α-KG treated worms (day 2, *P* = 0.969; day 8, **P* = 0.012; by *t*-test, two-tailed, two-sample unequal variance). Decreased oxygen consumption rates in (**f**) octyl α-KG treated cells (****P* = 0.0004, *****P* < 0.0001; by *t*-test, two-tailed, two-sample unequal variance) and (**g**) α-KG treated worms (*P* < 0.0001; by *t*-test, two-tailed, two-sample unequal variance). RLU, relative luminescence unit. **h**, α-KG, released from octyl α-KG (800 μM), decreases state 3, but not state 4o or 3u (*P* = 0.997), respiration in mitochondria isolated from mouse liver. The respiratory control ratio is decreased in the octyl α-KG (3.1 ± 0.6) vs. vehicle (5.2 ± 1.0) (**P* = 0.015; by *t*-test, two-tailed, two-sample unequal variance). **i**, Eadie-Hofstee plot of steady-state inhibition kinetics of ATP synthase by α-KG (produced by *in situ* hydrolysis of octyl α-KG). [*S*] is the substrate (ADP) concentration, and *V* is the initial velocity of ATP synthesis in the presence of 200 μM octanol (vehicle control) or octyl α-KG. α-KG (produced from octyl α-KG) decreases the apparent V_{max} (53.9 to 26.7) and K_m (25.9 to 15.4), by nonlinear regression least squares fit. Number of independent experiments, c–i: 2. Mean ± s.d. is plotted in all cases.

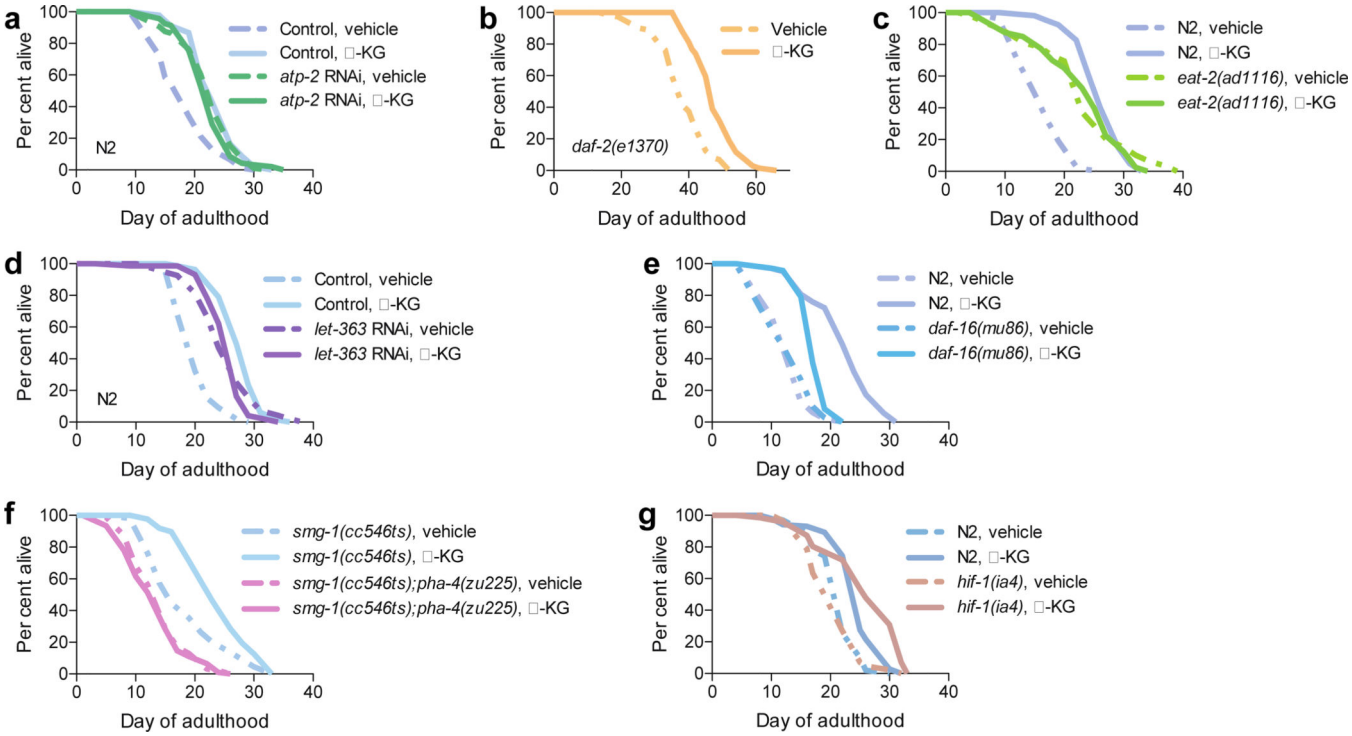

Figure 3. α-KG longevity is mediated through ATP synthase and the DR/TOR axis

Effect of α-KG on the lifespan of mutant or RNAi worms: **a**, *atp-2(RNAi)*, m_{veh} = 22.8 (n = 97), $m_{\alpha\text{-KG}}$ = 22.5 (n = 94), P = 0.35; or RNAi control, m_{veh} = 18.6 (n = 94), $m_{\alpha\text{-KG}}$ = 23.4 (n = 91), P < 0.0001. **b**, *daf-2(e1370)*, m_{veh} = 38.0 (n = 72), $m_{\alpha\text{-KG}}$ = 47.6 (n = 69), P < 0.0001. **c**, *eat-2(ad1116)*, m_{veh} = 22.8 (n = 59), $m_{\alpha\text{-KG}}$ = 22.9 (n = 40), P = 0.79. **d**, *CeTOR(RNAi)*, m_{veh} = 25.1 (n = 96), $m_{\alpha\text{-KG}}$ = 25.7 (n = 74), P = 0.95; or *gfp* RNAi control, m_{veh} = 20.2 (n = 99), $m_{\alpha\text{-KG}}$ = 27.7 (n = 81), P < 0.0001. **e**, *daf-16(mu86)*, m_{veh} = 13.4 (n = 71), $m_{\alpha\text{-KG}}$ = 17.4 (n = 72), P < 0.0001; or N2, m_{veh} = 13.2 (n = 100), $m_{\alpha\text{-KG}}$ = 22.3 (n = 104), P < 0.0001. **f**, *pha-4(zu225)*, m_{veh} = 14.2 (n = 94), $m_{\alpha\text{-KG}}$ = 13.5 (n = 109), P = 0.55. **g**, *hif-1(ia4)*, m_{veh} = 20.5 (n = 85), $m_{\alpha\text{-KG}}$ = 26.0 (n = 71), P < 0.0001; or N2, m_{veh} = 21.5 (n = 101), $m_{\alpha\text{-KG}}$ = 24.6 (n = 102), P < 0.0001. m, mean lifespan (days of adulthood); n, number of animals tested. P-values were determined by the log-rank test. Number of independent experiments: RNAi control (6), *atp-2* (2), *CeTOR* (3), *N2* (5), *daf-2* (2), *eat-2* (2), *pha-4* (2), *daf-16* (2), *hif-1* (5).

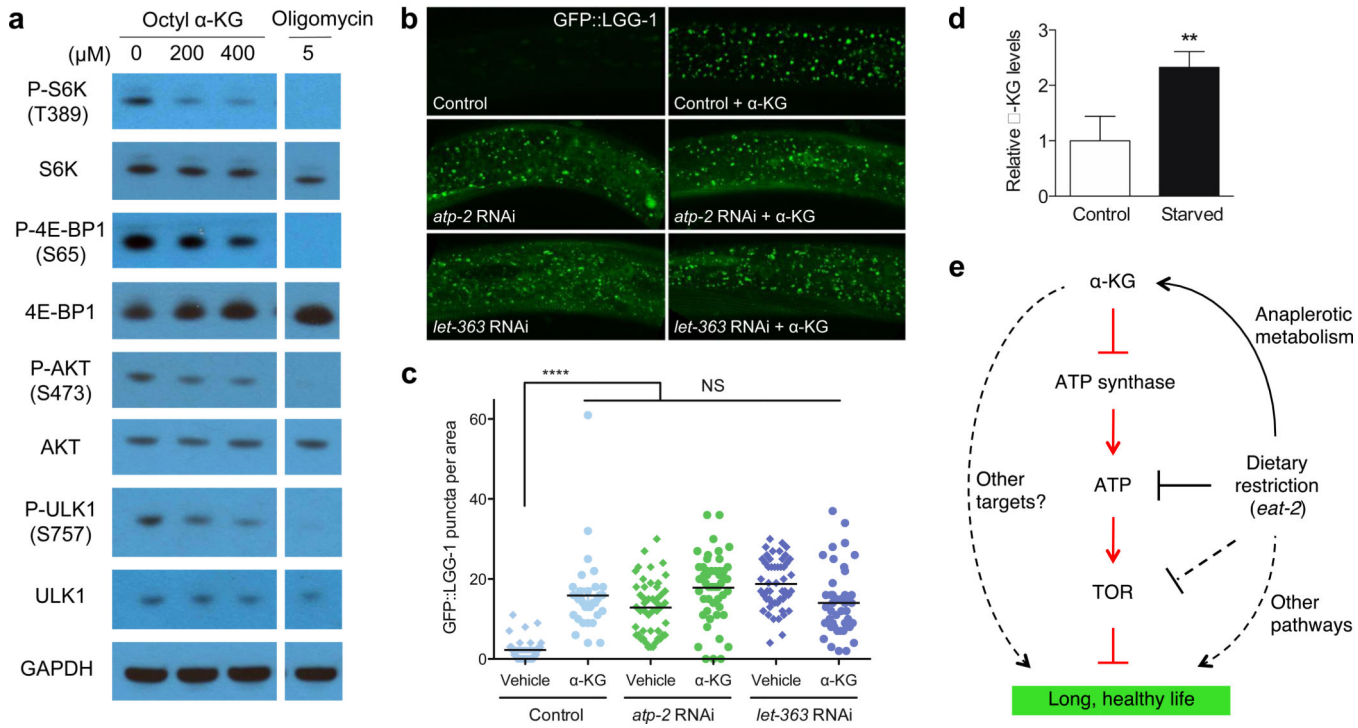

Figure 4. Inhibition of ATP synthase by α-KG causes conserved decrease in TOR pathway activity

a, Decreased phosphorylation of mTOR substrates in U87 cells treated with octyl α-KG or oligomycin. Similar results were obtained in HEK-293, normal human fibroblasts, and MEFs (not shown). **b**, Increased autophagy in animals treated with α-KG or RNAi for *atp-2* or *CeTOR*. **c**, GFP::LGG-1 puncta quantitated using ImageJ (Methods). 2–3 independent experiments. Bars indicate the mean. ****$P < 0.0001$; n.s., not significant (*t*-test, two-tailed, two-sample unequal variance). **d**, α-KG levels are increased in starved worms. **$P < 0.01$ (*t*-test, two-tailed, two-sample unequal variance). Mean ± s.d. is plotted. **e**, Model of α-KG-mediated longevity.